

**MECHANISM OF BBB PERMEABILITY ENHANCEMENT IN RABIES VIRUS
INFECTION**

by

QINGQING CHAI

(Under the Direction of Zhen F. Fu)

ABSTRACT

Infection with laboratory-attenuated rabies virus (RABV) enhances Blood-brain Barrier (BBB) permeability, which has been demonstrated to be an important factor for host survival, since it allows immune effectors to enter the central nervous system (CNS) and clear RABV. To probe the mechanism by which RABV infection enhances BBB permeability, the expressions of tight junction (TJ) proteins in the CNS were investigated following intracranial inoculation with laboratory-attenuated or wild-type (wt) RABV. BBB permeability was significantly enhanced in mice infected with laboratory-attenuated, but not wt, RABV. The expression levels of TJ proteins were decreased in mice infected with laboratory-attenuated, but not wt, RABV, suggesting that enhancement of BBB permeability is associated with the reduction of TJ protein expression in RABV infection. Brain extracts prepared from mice infected with laboratory-attenuated, but not wt, RABV reduced TJ protein expression in BMECs. It was found that brain extracts from mice infected with laboratory-attenuated RABV contained significantly higher

levels of inflammatory chemokines/cytokines than those from mice infected with wt RABV. Pathway analysis indicates that type II interferon (IFN- γ) is located in the center of the cytokine network in the RABV-infected mouse brain, and neutralization of IFN- γ reduced both the disruption of BBB permeability *in vivo* and the down-regulation of TJ protein expression *in vitro*. These findings indicate that the enhancement of BBB permeability and the reduction of TJ protein expression are not due to RABV infection per se but due to virus-induced inflammatory chemokines/cytokines.

Among these chemokines/cytokines, IFN- γ expression was detected in the late stage of RABV infection. However, chemokine CXCL10 was found to be the most highly and earliest expressed after infection with laboratory-attenuated RABV, it is hypothesized that CXCL10 could be the initiation factor for reduction in TJ protein expression and enhancement of BBB permeability. Therefore the temporal and spatial expression of CXCL10 was determined in the mouse brain after infection with RABV. Expression of CXCL10 was initially detected in neurons as early as day 3 post infection before it was detected in microglia (day 6 pi) and astrocytes (day 9 pi) in RABV-infected mice. Neutralization of CXCL10 reduced IFN- γ production, Th17 cell infiltration, loss of TJ protein expression, and the enhancement of BBB permeability in mice infected with laboratory-attenuated RABV. Thus neuronal CXCL10 induced by RABV initiates cascades leading to expression of other inflammatory chemokines/cytokines and enhancement of the BBB permeability.

INDEX WORDS: Rabies virus (RABV), Blood-brain Barrier (BBB), Tight junction (TJ) proteins, Chemokine, Cytokine, IFN- γ , CXCL10

**MECHANISM OF BBB PERMEABILITY ENHANCEMENT IN RABIES VIRUS
INFECTION**

by

QINGQING CHAI

Doctor of Veterinary Medicine, Huazhong Agricultural University, Wuhan, China, 2010

A Dissertation Submitted to the Graduate Faculty of The University of Georgia in Partial
Fulfillment of the Requirements for the Degree

DOCTOR OF PHILOSOPHY

ATHENS, GEORGIA

2014

© 2014

QINGQING CHAI

All Rights Reserved

**MECHANISM OF BBB PERMEABILITY ENHANCEMENT IN RABIES VIRUS
INFECTION**

by

QINGQING CHAI

Major Professor

Zhen F. Fu

Committee

Elizabeth W. Uhl

Nicolay M. Filipov

Matthew J. Sylte

Jason A. Zastre

Electronic Version Approved:

Julie Coffield

Interim Dean of the Graduate School

The University of Georgia

August 2014

DEDICATION

I dedicate this dissertation to my mom and dad, friends and mentor for providing me emotional and scientific support throughout my entire graduate school experience

ACKNOWLEDGEMENTS

First and foremost I would like to acknowledge my advisor, Zhen Fu, for providing resources and excellent training to conduct this research and preparing me with the tools to be a successful scientist. He has provided never-ending enthusiasm for my project and inspired me in my growth as a scientist. I also want to thank everyone in my committee for all their helpful advice over these years.

I would like to also thank all the members in the Fu lab, past and present, Ming Zhou for his help with the *in vivo* assays while studying in the lab, Clement Gnanadurai for his suggestions on how to communicate with collaborators, Drs. Wenqi He and Ruiping She for the advice on techniques during their visits. I would also like to thank everyone in the Pathology department, Drs. Buffy Howerth and Melinda Camus for patient guidance on utilizing departmental core facilities, Megan, Jennifer and Christy for offering help and kind words during all the time I was in the department.

Thank you to my family for always listening and being interested in what I was doing even if they did not understand a word I said. Finally, enormous thanks to Jenny, Janet, Nick, Pernilla, Rob, Anna for sharing laughter and friendship through all big and small days.

TABLE OF CONTENTS

	Page
ACKNOWLEDGEMENTS.....	v
CHAPTER	
1. INTRODUCTION.....	1
2. LITERATURE REVIEW	
I. Rabies Virus Structure And Replication.....	3
II. Host Responses To Rabies Virus Infection.....	7
III. Structure And Properties Of The Blood-brain Barrier.....	13
IV. Mechanisms Of Blood-brain Barrier Disruption In Diseases.....	17
V. References.....	24
3. ENHANCEMENT OF BLOOD-BRAIN BARRIER PERMEABILITY AND REDUCTION OF TIGHT JUNCTION PROTEIN EXPRESSION ARE MODULATED BY CHEMOKINES/CYTOKINES INDUCED BY RABIES VIRUS INFECTION	
I. Abstracts.....	43
II. Instruction.....	44

III. Materials & Methods.....	46
IV. Results.....	53
V. Discussion.....	60
VI. References.....	79

4. NEURONAL CXCL10 INITIATED INFILTRATION OF CD4+ T CELLS AND
ENHANCEMENT OF BLOOD-BRAIN BARRIER PERMEABILITY IN RABIES VIRUS
INFECTION

I. Abstracts.....	90
II. Instruction.....	91
III. Materials & Methods.....	92
IV. Results.....	97
V. Discussion.....	100
VI. References.....	109
5. SUMMARY AND DISCUSSION.....	114

CHAPTER 1

INTRODUCTION

Rabies is one of the oldest zoonotic diseases; it was recognized in Egypt since before 2300BEC and chronicled by Aristotle in Ancient Greece. Rabies virus (RABV) infects both humans and animals, and it causes 55,000 human fatalities annually worldwide. RABV targets exclusively neurons in the central nervous system (CNS), ultimately causes encephalomyelitis, paralysis and fatality. Pathogenesis of RABV infection was investigated by comparing the disparities of wild type (wt) and laboratory-attenuated RABVs induced effects on brains of infected animals. Minimal inflammation or neuronal apoptosis is found in brains of animals infected with high-virulence wt RABV, while low-virulence laboratory-attenuated RABV caused extensive inflammatory responses and neurodegeneration in brains of infected animals.

Enhancement of Blood-brain Barrier (BBB) permeability can be caused by various factors in bacterial and viral infections and autoimmune diseases, the current studies summarized in this dissertation were conducted to broaden the understanding of RABV pathogenesis and perspectives of BBB disruption in encephalitis. This dissertation begins with Chapter 2, a literature review comprised of four sections. Section I introduces structure and replication of

RABV. Section II covers host immune responses in the CNS caused by RABV infection. Section III includes structure and function of the BBB. Section IV contains mechanisms of BBB disruption caused by diseases. Chapters 3 and 4 each consists of manuscripts describing the results of studies comprising my dissertation research. Chapter 3 contains research that showed how RABV infection disrupted expressions of tight junction (TJ) proteins and BBB integrity. Chapter 4 includes research that investigated the factors initiating and amplifying enhancement of BBB permeability in RABV infection. The dissertation ends with Chapter 5 that provides a discussion of all my studies in this area.

CHAPTER 2

LITERATURE REVIEW

I. Rabies viral genome, proteins and replication

Rabies virus (RABV) is the prototype virus of the *Lyssavirus* genus in the *Rhabdoviridae* family, *Mononegavirales* order (1). The family *Rhabdoviridae* consists of more than 100 viruses causing diseases in vertebrates, invertebrates and plants and is known specifically for their rod- or bullet-shaped morphological appearance (2, 3). The two genera of the *Rhabdoviridae* family contain human pathogens of medical importance, consisting of vesicular stomatitis virus (VSV) from the *Vesiculovirus* genus, and RABV, the most important human pathogen in the *Lyssavirus* genus (4).

Rabies viral genome

Rabies virus is a negative-sense, single stranded RNA virus, containing a non-segmented genome of 12,000 bases (5, 6). The RABV genome contains 5 viral structural proteins in the order of nucleoprotein (N), a transcriptase-associated phosphoprotein (P, formerly called nonstructural protein, NS), matrix protein (M), glycoprotein (G), and RNA-dependent RNA polymerase (RdRp, also known as large protein, L). The N, P, and L proteins comprise the ribonucleoprotein (RNP) complex, which constitutes the active viral replication unit with the

viral single-stranded RNA (7). The RABV genome is flanked by a leader sequence at the 3'-hydroxyl end and a 5'-triphosphate trailer (5'-ppp), and genome is separated by four intergenic regions (Fig. 1.1).

RABV receptors and virus entry

Although RABV has been reported to enter all cell types, it only replicates in neurons. Infection and replication of RABV include virus attachment, entry, uncoating, transcription, translation, replication, assembly, and budding (8). Viral envelope attaches and fuses with receptors on the host cell membrane via G protein homotrimers. It has been shown that mutation of the G protein significantly reduced neuroinvasiveness both in cell cultures and animals, supporting the significance of G protein in RABV invasion (9). It has been proposed that p75 neurotrophin receptor (p75NTR), neural cell adhesion molecule (NCAM) and nicotinic acetylcholine receptor (NACHR) act as RABV-specific receptors (10). After attachment, pinocytosis of RABV particles by host cells occurs through the formation of clathrin-coated vesicles. RABV is then uncoated into RNP in large endosome and released into the cytoplasm in a pH-dependent manner and ready for the transcription and translation in the cytoplasm.

Transcription, translation, and assembly of RABV

Upon RABV infection, viral RNAs are transcribed and replicated inside cytoplasmic NBLs (negri body-like structures) of an infected neuron (11). The negative-stranded RNA of RABV is not capable of serving as a mRNA template or translating the vRNA(-) into essential transcriptase/replicase proteins, so RABV carries its own virus-encoded polymerase as an integral component of the viral particle. Uncoated RNP complex released in the cytoplasm contains genomic vRNA(-), N protein, and RABV polymerase (L/P proteins). L and P proteins

form a polymerase L-P complex during viral RNA synthesis, in which the enzymatic L protein and cofactor P protein bind to the N-RNA template, inducing a conformational change in order to position the polymerase on the template correctly for viral transcription. RABV transcription involves sequential production of monocistronic mRNAs by viral polymerase (L+P). The RABV polymerase attaches to the 3'-end of genome, and linear viral ssRNA genome is transcribed into capped and polyadenylated mRNA that permits translation using host cell machinery. The notable feature of RABV ssRNA transcription is that approximately 30% attenuation occurs at each intergenic gene junction, and only 70% of successive individual gene sequence is transcribed each time transcription is re-initiated at the intergenic boundary since 30% reinitiation fails to occur (6, 12). Therefore, a gradient of mRNA of RABV gene order is observed corresponding to the RABV gene order (N>P>M>G>L).

In order to assemble new RABV virions, full-length positive strand RNA is also needed as a template for generating a full-length negative-stranded RABV genome. Leader RNA is contained at the extreme 3'-end of the full-length positive RNA strand. Leader RNA is 47 nucleotides long and neither capped or polyadenylated, it's not part of any of other mRNA species but the full length position strand RNA in RABV replication. Newly synthesized N protein binds to the 5'-end sub-genome-length mRNA and polymerase by interacting with P protein, so that polyadenylation at 3'-end is prevented and transcription of full-length positive strand mRNA is enabled. Sub-genome-length mRNA continues transcription until the L gene. Translation of viral protein components occurs on the host's free ribosomes in cytoplasm, and post-translational modification is completed in the endoplasmic reticulum (ER) and Golgi

apparatus. Ratio of leader RNA to N protein decides the switch point from transcription to assembly (13).

RABVs assembly and budding

RNP core is generated as newly synthesized vRNAs are packed with N, P, and L proteins. Replication of the virus ends with newly assembled RABV particles budding off from the host's cell membrane, which is regulated by M protein associated with lipid viral envelope. The RABV M protein mediates the assembly of the RABV proteins into a functional unit capable of budding and infecting further living cells (14-16). M protein also functions in inhibiting viral transcription and promoting condensation of RNP at the budding site to complete the RABV bullet-shaped morphology. Unlike the intracellular M protein, G protein is not essential in virus budding, but its reversibility is capable of facilitating this process (17, 18). The benefits of reversible G protein conformations are that fusogenic conformation allows G protein to be transported through acid environments of ER and Golgi apparatus and enables G protein to recover the prefusion conformation before budding near the cell surface with a neutral pH. It has also been shown that L and P proteins can promote formation of bullet-shaped morphology via interaction with the bilayer-lipid viral envelope.

Animal reservoirs and RABV spread

Replication of RABV occurs in various reservoirs. Most mammals are susceptible to RABV, coyotes, raccoons, skunks, and foxes are reservoirs species (19). Bats are the ultimate reservoirs for RABV. However, dogs remain the most important reservoirs for rabies for humans in the developing countries of Asia and Africa (20). The virus is normally deposited into victim's muscle tissue through a bite and incubation period lasts from several weeks to several years in

the infected wound since the initial bite. Rare transmission routes such as organ transplantation, aerosol, and mucous membrane are also documented. Although RABV can enter almost all cell types, it is recognized as highly neurotropic virus infecting and replicating in the CNS. RABV binds to RABV-specific receptors on the surface of neuromuscular synapses and enter motor or sensory nerves of innervated muscle, and it then moves to the CNS via retrograde axonal transport through motor or sensory neurons, where the viral particles are transported along microtubules from the periphery to the CNS by a dynein motor complex (21). RABV travels along the neural axon at a rate of 50-100 mm per day (22). Clinical symptoms emerge once RABV starts to replicate in the central nervous system (CNS) and the disease reaches prodromal phase. The virus then moves from the brain down to the salivary glands, the major exit portal of viral particles in reservoir and rabid animals, supporting the detection of high amounts of virus in the original wound and saliva of infected victims (23).

II. Clinical Symptoms and host immune responses to RABV infection

RABV causes fatal disease in human and animals, attributing to 55,000 fatalities each year around the world (24). Stray dogs are the major transmitters of RABV between hosts around the world (25-27), although 90% of the cases in the USA reported to the Centers of Disease Control and Prevention (CDC) every year are associated with wild animals. Around 18,000 people are vaccinated annually due to exposures to rabid or potentially infected animals in

America. Prompt immunization after exposure is strongly suggested and can prevent the development of rabies after the possibility of infection (28).

Clinical symptoms of RABV infection

Mortality rate for clinical rabies is 100% once the virus invades the CNS, begins replication, and develops clinical symptoms in the host. Initial clinical symptoms of rabies include fever, headache, pain, itching, delirium, insomnia, malaise, gastrointestinal symptoms, and fatigue, usually lasting for 2 to 10 days. Prodromal phase of rabies is followed by neurological symptoms that include hydrophobia, seizure, disorientation, and hallucination. With onset of neurological symptoms, extensive replication of RABV occurs in the limbic system, ultimately causing loss of cortical control of behavior and subsequential aggression in the animal. Virus dissemination to the neocortex leads to paralysis, respiratory failure and eventually death (29-32).

Disparities between wt and laboratory-attenuated RABVs infections

Despite of long history of RABV infections both in human and animals, the pathogenesis of RABV infection is still unclear. It has been observed that wild type (wt) RABV and laboratory-attenuated act differently in hosts (33). Wt RABV causes fatalities in victims, while laboratory-attenuated RABV infection causes low morbidity and mortality. In order to study the pathogenesis of RABV, comparing acts of wild type (wt) and laboratory-attenuated RABV infections both *in vivo* and *in vitro* is widely utilized (33). In the brain of an experimental animal infected with wt RABV, no or little inflammation is observed (34, 35). This is partially due to the fact that the brain is an immune privileged organ and innate immunity in the brain remains minimal (36). It takes time to trigger an adaptive immune response initiated in the

periphery, acquiring a longer time interval for immune effectors to reach the CNS. It has been reported that blood-brain barrier (BBB) remains intact or slightly disrupted in wt RABV infected animals, which makes it more difficult for the immune effectors to cross the BBB and reach the brain to clear the wt RABV (33).

On the contrary, extensive immune response, neuronal apoptosis, and enhanced BBB permeability was observed in laboratory-attenuated RABV infected animals (37). Failure in enhancing the BBB permeability has been shown to result in fatality in animals infected with silver hair bat RABV (9). Research data have shown that immune effectors including virus neutralizing antibodies (VNA) in the brain were concurrently observed with rapid clearance of virus, which strongly supports the reason of higher survival rate in the laboratory-attenuated RABV infection (9, 38, 39). This is probably due to the high level of G protein expression in laboratory-attenuated RABV-infected animals (40, 41). It has been demonstrated that G protein is the major determinant for the induction of immune responses in laboratory-attenuated RABV infection (42), and it also has been shown that significantly higher levels of chemokines/cytokines are stimulated in animals infected with laboratory-attenuated, but not wt, RABV.

Recognition of RABV by host innate immunity

Host immune responses start with the recognition of RABV by host immune surveillance. Host immunity recognizes the RABV pathogen-associated molecular patterns (PAMPs) via pattern recognition receptors (PRRs), including toll like receptors (TLRs) on either surface or compartments of immune cells (43). TLRs expressed on monocytes, dendritic cells (DCs) and B cells are important sensors for induction of innate immunity (26). TLRs 2/4 sense

contribute to antiviral immunity in RABV-infected host by targeting heat shock proteins (HSPs) expressed by infected cells (11). It has also been shown that the cytoplasmic retinoic acid inducible gene-1 like helicase (RIG-1) and endosomal transmembrane TLRs 3/7/8 recognize RABV vRNA in infected neurons, further inducing production of type 1 Interferon (IFN- α/β) and other inflammatory cytokines (44-46). Signaling through TLRs is mediated by adaptor protein MyD88 in activating downstream transcription factors such as nuclear factor- κ B (NF κ B) and IFN regulatory factors (IRFs). It has been demonstrated that MyD88 plays a critical role in protecting host in RABV infection since MyD88^{-/-} mice infected with laboratory-attenuated RABV showed 100% mortality, indicating that MyD88 acts as an essential component in activating immune response in laboratory-attenuated RABV infection (47).

Role of chemokines/cytokines in RABV infection

It has been shown that expression of chemokines/cytokines plays an important role in laboratory-attenuated RABV infection; this is because their function is to recruit immune cells along the chemokines/cytokines gradient into the CNS (48). Therefore, virus can be cleared by leukocytes infiltrated in the CNS and the host can be rescued from established infection (49). It has been demonstrated that immune cells express chemokines/cytokines, but the brain resident cells are also shown to be the sources for chemokines/cytokines (50-52).

Activated by the signal from TLRs, NF κ B and IRFs promote the expression of pro-inflammatory cytokines, such as TNF and IFN genes (53). IFN is produced rapidly following exposures to wide range of pathogens; it is considered as an early defense of innate immunity. Antiviral ability of IFN system has been proven to play an important role in RABV infection (54). IFN- α/β suppress RABV replication and drive neighboring cells of infected tissue into

antiviral status, as well as recruit leukocytes into the infected tissue by initiating production of chemokines. It has been shown that IFN- α/β also initiates adaptive immunity by activating macrophages and DCs. Besides the signaling pathways initiated by TLRs activation, pro-inflammatory chemokines/cytokines can also be expressed through the JAK/STAT signaling transduction pathway following stimulation of Type II IFN (IFN- γ)-stimulated genes (ISGs) (55).

Among all the chemokines/cytokines, CXCL10 has been demonstrated to be one of the mostly expressed chemokines. CXCL10 is a chemokine identified as an IFN- γ stimulated protein (56). CXCL10 and IFN- γ have been shown to function in RABV infection and will be further discussed in chapter three and four of this dissertation. CXCL10 can be produced by a collection of cells in inflamed tissues, including ECs, macrophages, fibroblasts, keratinocytes, neurons, and activated T cells (57). *In vitro* study has shown that macrophages stimulated with UV-inactivated RABV activate the extracellular signal-regulated kinase 1/2 (ERK1/2), which subsequently induced the expression of CXCL10 in macrophages (58). It has been shown that CXCL10 is one of the most potent chemoattractants among all chemokines, it is hypothesized that leukocytes migrate to the CNS following a CXCL10 gradient in the RABV infection. Recruited T cells in the CNS recognize RABV and express IFN- γ that magnifies CXCL10 production, leading to initiation of a full-blown inflammatory response (59).

Wt-RABV evades host immune response and surveillance

It has been shown that recruitment of immune cells and production of antiviral chemokines/cytokines are important in restraining RABV infection in animals. However, RABV has evolved several strategies to evade the immune surveillance after infecting neurons of

different species for thousands of years (23). It has been shown that N protein is associated with the evasion of RIG-I-mediated antiviral effect. P protein has been reported as an IFN antagonist in RABV infection by inhibiting the phosphorylation of IRF3 and IRF7 by kinases TBK-1 and TKKi (60). P protein has also been shown to be capable of blocking the JAK/STAT signaling pathway, so that the nuclear import of IRF 3/7 and STAT/IRF9 are restrained and downstream antiviral IFN production and activity are blocked. TLR3 is sequestered in Negri bodies (NBL) in infected neurons, preventing antigen sensor TLR3 from activating or triggering innate immunity (61).

Apoptosis occurred in immune cells stimulated by RABV is considered to be one route in which RABV evades immune surveillance (62). Apoptosis has been found in infiltrated leukocytes, which limit the RABV viral load, reduce CNS inflammation, and is considered highly beneficial to the host (63). Apoptotic CD3⁺ T cells have been observed in brain and spinal cord slices derived from hosts infected with encephalitic CVS RABV strain. It has also been found that RABV is capable of inducing the expression of HLA-G on surface of infected neurons, and interacting with HLA-G ligand on infected neurons has been demonstrated to be the trigger of death signaling in activated T cells (9, 64, 65). It has been shown that highly expressed G protein is capable of stimulating apoptosis in neurons in infected animals (40). This is one of the main reasons why low morbidity and mortality was observed in animals infected with attenuated RABV.

III. Structure and properties of the Blood-brain Barrier

The BBB is the most extensively distributed barrier and encompasses the largest surface area of the brain (66). One of the notable features is that integrity of BBB is disrupted in laboratory-attenuated RABV infection, while this is not observed in animals infected with wt RABV. It has been hypothesized that BBB plays a critical role in RABV clearance (9). Disruption of BBB integrity allows the immune effectors including antibodies and lymphocytes to enter the CNS, clear the virus, and rescue the infected animals from established infections (67). In contrast, intact BBB in wt RABV-infected animal prevents the entry of immune effectors, so that clinical symptoms occur when virus begins uncontrolled replication in the CNS and fatality becomes inevitable.

Discovery and functions of the BBB

The concept of the BBB arose from a study conducted by Hugh Davson in 1967 (68). It was found that an albumin-specific dye injected into the blood circulation failed to stain a normal brain. An injection of bile acid given into the brain generated seizures, but was unsuccessful in generating seizures when injected directly into the peripheral blood circulation (69). As a result of Davson's research, BBB is considered a non-static, physical, and monocellular transport barrier separating the peripheral circulation from the CNS, providing a controlled and specific metabolic source directly to the CNS alone.

Precisely regulated maintenance of the microenvironment is necessary for maintaining proper functions of the CNS and preventing leakage to and from the brain is the basic necessary

characteristic (70). The BBB prevents xenobiotic, toxic metabolites, and peripheral immune cells from entering the CNS, as well as limiting the paracellular entry of hydrophilic molecules from blood circulation (71). It, however, allows small lipophilic molecules, including CO₂ and O₂, to diffuse across the endothelium and enter the CNS along the concentration gradient. The BBB supplies nutrients to the CNS and regulates the efflux of waste products. Essential nutrients such as glucose and amino acids enter the brain via transporters on the surface of endothelium at the BBB. Uptake of large molecules by the brain, such as insulin, leptin, iron and transferrin are mediated by receptors on endothelial cells (ECs) (70).

The BBB selectively transports several types of chemokines/cytokines, promoting pro-inflammatory response in the brain (72, 73). A few of these include IL-1 α , IL-1 β , IL-6, TNF, epidermal growth factor (EGF), and Leukemia-inhibiting factor (LIF) used in routine physiological response to inflammation and neuroregeneration, while TGF-1 α and TGF-1 β are strictly prevented from entering the brain (74). Chemokines/cytokines in the CNS can interact with each other to mediate the TJ protein formation and EC signaling, which consequently generate the secondary signals that modulate function within the CNS (72).

TJ proteins in ECs at the BBB

Most studies on BBB properties focus on brain endothelium, the largest surface area of the BBB. Endothelium is comprised of ECs that are the major component of the BBB (75). There are adherens junctions (AJ) and TJ proteins locating between adjacent ECs that control BBB permeability (66, 76). The junctional protein complex between adjacent ECs acts as a physical selective barrier, because it forces the majority of the molecules to take the transcellular route (via channels or transporters) when moving from the periphery to the CNS (77). Therefore,

molecules that are transported between blood circulation and the CNS are strictly controlled by TJ proteins in order to protect the CNS environment (72).

TJ proteins contain integral transmembrane proteins and cytoplasmic membrane proteins. Transmembrane TJ proteins include junctional adhesion molecules (JAM)-A/B/C, endothelial cell-selective adhesion molecules (ESAM), a coxsackie and adenovirus receptor (CAR), and claudins 3/5/12 and occludin, which connect with the intracellular scaffolding proteins zonular occludens (ZO) 1/2/3 (66, 78-80). External loops, carboxy (C)-terminal domain, of claudin and occludin regulate intercellular adhesions by interacting with the same proteins of neighboring ECs (81). Claudins are 22kDa and have four transmembrane domains. They are the major components of TJ protein strands and mediate various BBB properties. It has been shown that claudin 3/5/12 collectively contribute to high transendothelial electrical resistance (TEER) when executed together. Occludin is a 60-kDa integral membrane phosphoprotein with four transmembrane segments, containing both the carboxy terminus and amino terminus intracellularly (82). It has been demonstrated that most of the occludin is expressed in the brain ECs, more than any other nonneuronal tissue (83). ZO-1, a 220-kDa phosphoprotein, was the first component of TJ proteins identified (81). The COOH region of ZO-1/2/3 bind to the cytoplasmic domain of the transmembrane TJ proteins and interacts with actin cytoskeletons, creating a cytoplasmic plaque collectively termed membrane-associated guanylate-kinase-like protein (MAGUKs) (81).

Other cell components of the BBB

Brain endothelium shows a much lower degree of transcytosis and endocytosis than peripheral endothelium. Various components make up the BBB in addition to brain ECs: basal

lamina, pericytes, microglial cells, and astrocytic end-feet with the basement membrane covering the vessel wall (73). Altogether these components create a dynamic and multi-cellular component called the neurovascular unit (NVU) (66, 81, 84). Pericytes are the least studied component of the BBB (85) and have been shown to be involved in structural integrity, angiogenesis, differentiation of vessel, and formation of TJ proteins (86, 87). Astrocytes play a role in BBB maintenance and contribute to the formation of glial limitans, which functions as a support for EC basal lamina and astrocytic end-feet (88). Astrocytes have also been shown to be important in developing properties of the BBB (75). Previous *In vitro* studies showed that ECs co-cultured with astrocytes or astrocyte-conditioned media possessed high TEER levels, while other neuronal and non-neuronal tissue developed no such properties (89). In diseases with damaged BBB, vascular endothelial growth factor (VEGF) and other cytokines secreted by astrocytes also contribute to enhancing the BBB permeability (90).

Agents that regulate the BBB permeability

Alterations of either AJ or TJ proteins in ECs contribute to the disruption of BBB integrity and brain function in disease conditions (91). Breakdown of the BBB results in brain edema and allows infiltration of leukocytes and exogenous molecules, thereby significantly increasing CNS inflammation (92). It has been shown that BBB permeability is modulated by various factors. Agents tightening the BBB include steroids, elevated intracellular cyclic AMP (cAMP), adrenomedulin and noradrenergic agents (93). Some of these agents are expressed by ECs such as endothelin-1, but others are expressed by other cell components of the BBB, infiltrated immune cells, or other resident brain cells (92). Agents that regulate brain endothelial function and impair BBB constraint have also been identified. Molecules that impair BBB

function include bradykinin, histamine, serotonin, glutamate, purine nucleotides, adenosine, platelet-activating factor, interleukin (IL)-1 α , IL-1 β , IL-6, TNF- α , macrophage-inhibitory proteins-1/2 (MIP-1/2, also called CCL3/CXCL2), free radicals, nitric oxide (NO), prostaglandins, ATP, quinolinic acid, and leukotrienes (93).

IV. Mechanisms of blood-brain barrier disruption in disease

Disruption of BBB integrity in physiological and pathological conditions

In some physiological conditions, expression of inflammatory products by immune cells enhances BBB permeability accumulatively (72). For instance, hypoxia-ischemic insult of the brain induces resident brain cells to produce AMs (ICAMs) and inflammatory factors (IL-1 β , CCL2, TNF- α , and IL-8) (92). It has been shown that neutrophils attached to ICAMs on the surface of ECs infiltrate the CNS and subsequently disrupt the BBB hypoxia-ischemia insulted brain (94).

BBB disruption is often observed in many pathological conditions, such as with infections of neurotropic viruses. For instance, BBB disruption is observed in Japanese Encephalitis virus (JEV) and WNV infections (95). It has been observed that both JEV and WNV infections enhanced BBB permeability. Enhancement of BBB permeability has been well investigated in MS, experimental autoimmune encephalomyelitis (EAE), infection of human immunodeficiency virus (HIV), mouse adenovirus type-1 (MAV-1), and malaria (96). It has been shown that enhancement of BBB permeability in some pathological conditions is associated with the expression of matrix metalloproteinase (MMP). MMP is capable of degrading the basal

lamina of endothelium, which leads to opening of parenchymal basement membrane and allows the entering of leukocytes. For instance, herpes simplex virus (HSV-1) causes encephalitis through a neuronal route, and increased activity of MMPs 2/9 has been found concurrently with disrupted BBB in HSV-1-infected mouse model (97). In addition to MMP, chemokines, cytokines, free radicals, vasogenic factors, and lipid mediators were also capable of modulating BBB permeability in various pathological conditions (96).

Direct disruption of BBB by pathogens

A few pathogens cause severe and direct damage to the BBB integrity during their replications in hosts, such as parasites of *Plasmodium spp*, *Toxoplasma gondii*, and *trypanosomes* (98-101). It has been shown that viral infections can also cause direct damage to ECs at the BBB. Enhancement of BBB permeability, decreased TEER, and reduction of TJ proteins are found in MAV-1 infections (102). It has been observed that infection of MAV-1 in the brain is restricted within the perivascular region, so the spread of the virus is due to a direct damage to the viability of endothelium at the BBB (103-105). It has also been demonstrated that BBB disruption is independent of the brain inflammation in MAV-1 infection. Histopathological evidence found in brain vasculature involving MAV-1 infection strongly supports the hypothesis that disruption of the BBB integrity is caused by direct damages in MAV-1 infection (102).

Indirect disruption of BBB by pathogens

In most diseases, enhancement of BBB permeability is due to indirect damages to TJ proteins at the BBB caused by pathogen gene products or infiltration of immune effectors in the CNS. WNV infection is characterized by neuronal inflammation, neuronal loss and BBB disruption. It has been shown that reductions of TJ proteins (ZO-1, occludin, claudin, and β -

catenin) were observed when replication of WNV and inflammation occurred (106). It has been demonstrated that WNV infection causes BBB disruption through the TLR3-dependent inflammatory response (107, 108), and it has been shown that chemokines/cytokines including CCL5 and CXCL10 play a critical role in BBB disruption in WNV infection (109, 110). In addition, TJ protein levels are reduced in ECs co-cultured with supernatants collected from MHV-infected astrocytes, it was hypothesized that this is probably due to the MHV-induced VEGF expression derived from astrocytes (111).

Also, the indirect disruption of BBB has been shown in HIV infection. It has been found that HIV proteins, such as Tat, gp120, and Nef, contribute to changes in the BBB integrity (96). Tat has been shown to interact with ECs, and together they activate inflammation and stimulate the expression of AMs and MMP9 enzyme proteolytic activity (112). Expressions of MMP2 and MMP9 are also increased in HIV-infected *in vitro* model of the BBB, which strongly supports the hypothesis that Tat-induced expressions of MMPs are associated with BBB disruption in HIV. In addition, it has been found that expression of occludin can be inhibited by expression of Tat protein through the Rho-A signaling pathway (113). Gp120 is a viral glycoprotein, and it has been demonstrated that increased expressions of MMP 2/9 are associated with decreased expressions of claudin-5 and basal lamina in rat receiving injection of gp120 (114). Oxidative stress also contributes to gp120 stimulated BBB disruption, but the mechanism is unclear. Nef is the third HIV protein that has been shown to be capable of damaging the BBB. Production of Nef is responsible for the alteration of astrocytes end feet formation, contributing to elevated brain inflammation, increased sensitivity of astrocytes to reactive oxygen species (ROS), and disruption of BBB integrity (115).

BBB disruption by infection-induced expression of chemokines/cytokines.

It has been shown that inflammatory mediators play an important role in reducing the TJ protein expression and enhancing the BBB permeability in pathological conditions. Studies have shown that the productions of chemokines/cytokines stimulated in diseases are proven to be critical in BBB permeability changes (116). For instance, it has been demonstrated that CCL2 expressed by monocytes is essential in BBB disruption in HIV infection (117). With an absence of CCL2, less BBB disruption, reduction of TJ proteins, decreased infiltration of immune cells and expression of MMP2/9 are observed in HIV infected animals. Function of CCL2 on BBB has also been studied via *in vitro* model system, showing that incubation with CCL2 causes altered expression of ZO 1/2, occludin, and claudin-5 (118). In addition, CCL2 has been demonstrated to be a primary chemoattractant for monocytes (119-121), which may contribute to the amplification of BBB disruption in HIV infection.

Chemokines/cytokines can be expressed by immune cells, and it has been shown that brain resident cells, including neurons, microglia, and astrocytes, are also sources of chemokines/cytokines. It has been shown that CXCL10 produced in neurons enhanced BBB permeability in WNV infection (110). IL-6 produced by astrocytes can amplify the opening of TJs (75). Obesity stimulated enhancement of BBB permeability is associated with activation of microglia, and primary microglia isolated from aged animals also show exacerbated oxidative stress (122). In hypoxic-ischemia brains, VEGF expressed by astrocytes has been proven to enhance the gap formation and cause enhanced permeability of the endothelium, neutralization of VEGF-A expression significantly reduces the enhancement of BBB permeability (90, 123).

Effect of CXCL10 on BBB disruption

In RABV infection, it has been observed that substantial levels of CXCL10, CCL5, and CCL3 were expressed in laboratory-attenuated RABV-infected mice. It has also been shown that enhancement of BBB permeability is associated with expression of CXCL10, CCL5, and CCL3. Infection of recombinant RABV expressing CXCL10 in mice showed significantly more enhancement of BBB permeability and reduction of TJ proteins than infections of recombinant RABVs expressing others two chemokines (116, 124). It has been hypothesized that CXCL10 is essential in enhancement of BBB permeability in laboratory-attenuated RABV infection.

CXCL10 is an IFN- γ inducible protein expressed by neurons, macrophages, astrocytes, CD14⁺ monocytes, T cells and ECs (117). It has been shown that WNV-infected cerebellum granule neurons are the primary sources expressing CXCL10 (110). However, microglia and astrocytes can also be source for CXCL10, most notably in neurotropic viruses of MHV, HIV, Theiler's virus, and herpes simplex virus (HSV). CXCL10 is a potent chemoattractant for activated T cells and NK cells (125). CXCR3 expressed on T cells is the cell surface receptor for CXCL10. Expression of CXCL10 efficiently recruits macrophages, T cells, NK cells and control the CNS viral loads of MHV, HSV and WNV infections (126). It has been demonstrated that neutralization of CXCL10 successfully prevented BBB degradation and protected T cells from entry into the CNS during an early stage MHV infection (127). However, in late stage MHV infection, CXCL10 is proven to be responsible for influx of immune cells, CNS inflammation, and demyelination of neurons, resulting in substantial expression of chemokines/cytokines in the CNS and further enhancement of BBB permeability (128).

Therefore, functions of CXCL10 can be stimulating enhancement of BBB permeability and amplify the positive feedback of BBB disruption in viral infections.

However, the impact of CXCL10 on the host in EAE is complex. Neutralization of CXCL10 in an EAE animal model showed reduced BBB disruption and less infiltration of immune cells in the CNS, resulting in amelioration of clinical symptoms with improved histological signs (129). A study of EAE using CXCL10^{-/-} animals showed less improvement, which might be due to compensation by CXCL 9/11 expressions (130). CXCL 9/11 share the same cell surface receptor with CXCL10 and are induced by IFN- γ , as well as in various cell types.

Recent research on BBB offers us a better understanding of BBB morphology and physiology, as well as an insight into the development and treatment of certain brain diseases (131). These findings suggest that various mechanisms of BBB disruption can be caused by different effectors, both generated from peripheral blood circulation and host residential brain cells. Further investigation involving the mechanisms of BBB disruption in RABV infection in the present study provides us a better understanding of both BBB function and pathogenesis of RABV infection.

Hypotheses of mechanisms used by RABV in disrupting BBB integrity

Based on extensive study of BBB disruption in viral infections, we hypothesized that enhancement of BBB permeability is associated with reductions of TJ proteins in RABV infection. Because neurons are the exclusive targets for RABV infection, so the hypothesis for the second phase of the present study is that expression of CXCL10 induced by RABV infection initiates a cascade of chemokines/cytokines production and BBB disruption.

Fig 1.1

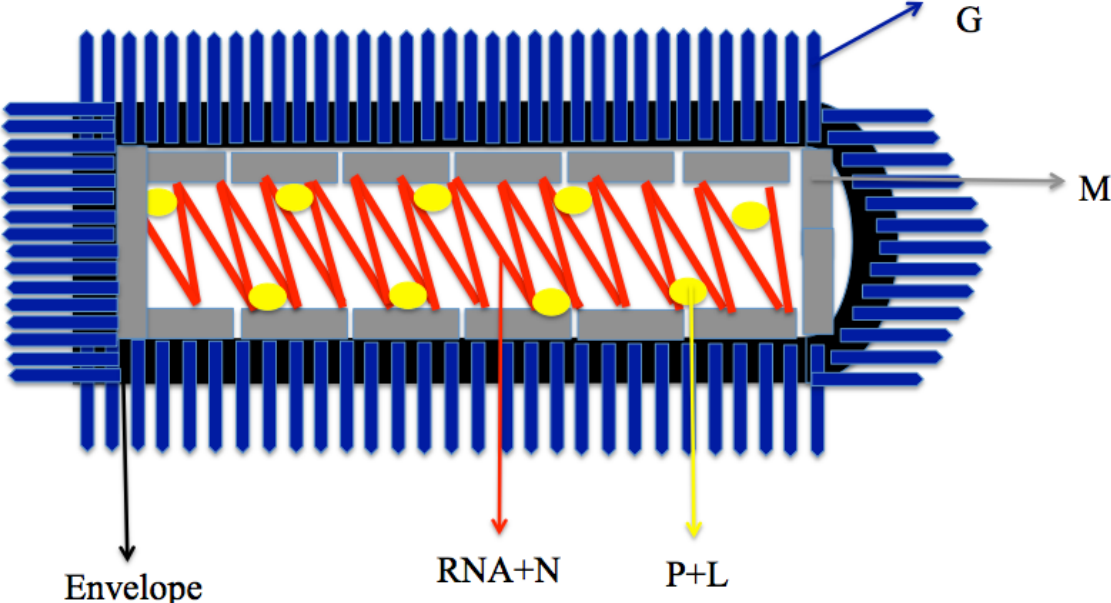


Fig. 1.1. Structure of RABV

V. References

1. **Schneider LG, Diringer H.** 1976. Structure and molecular biology of rabies virus. *Current topics in microbiology and immunology* **75**:153-180.
2. **Rieder M, Conzelmann KK.** 2011. Interferon in rabies virus infection. *Advances in virus research* **79**:91-114.
3. **Ge P, Tsao J, Schein S, Green TJ, Luo M, Zhou ZH.** 2010. Cryo-EM model of the bullet-shaped vesicular stomatitis virus. *Science* **327**:689-693.
4. **Rupprecht CE, Hanlon CA, Hemachudha T.** 2002. Rabies re-examined. *The Lancet infectious diseases* **2**:327-343.
5. **Matsumoto S.** 1962. Electron microscopy of nerve cells infected with street rabies virus. *Virology* **17**:198-202.
6. **Albertini AA, Ruigrok RW, Blondel D.** 2011. Rabies virus transcription and replication. *Advances in virus research* **79**:1-22.
7. **Schnell MJ, McGettigan JP, Wirblich C, Papaneri A.** 2010. The cell biology of rabies virus: using stealth to reach the brain. *Nature reviews. Microbiology* **8**:51-61.
8. **Okumura A, Harty RN.** 2011. Rabies virus assembly and budding. *Advances in virus research* **79**:23-32.
9. **Roy A, Phares TW, Koprowski H, Hooper DC.** 2007. Failure to open the blood-brain barrier and deliver immune effectors to central nervous system tissues leads to the lethal outcome of silver-haired bat rabies virus infection. *Journal of virology* **81**:1110-1118.

10. **Tuffereau C, Schmidt K, Langevin C, Lafay F, Dechant G, Koltzenburg M.** 2007. The rabies virus glycoprotein receptor p75NTR is not essential for rabies virus infection. *Journal of virology* **81**:13622-13630.
11. **Lahaye X, Vidy A, Pomier C, Obiang L, Harper F, Gaudin Y, Blondel D.** 2009. Functional characterization of Negri bodies (NBs) in rabies virus-infected cells: Evidence that NBs are sites of viral transcription and replication. *Journal of virology* **83**:7948-7958.
12. **Wertz GW, Perepelitsa VP, Ball LA.** 1998. Gene rearrangement attenuates expression and lethality of a nonsegmented negative strand RNA virus. *Proceedings of the National Academy of Sciences of the United States of America* **95**:3501-3506.
13. **Vidal S, Kolakofsky D.** 1989. Modified model for the switch from Sendai virus transcription to replication. *Journal of virology* **63**:1951-1958.
14. **Lenard J, Vanderoef R.** 1990. Localization of the membrane-associated region of vesicular stomatitis virus M protein at the N terminus, using the hydrophobic, photoreactive probe 125I-TID. *Journal of virology* **64**:3486-3491.
15. **Mebatsion T, Weiland F, Conzelmann KK.** 1999. Matrix protein of rabies virus is responsible for the assembly and budding of bullet-shaped particles and interacts with the transmembrane spike glycoprotein G. *Journal of virology* **73**:242-250.
16. **Zakowski JJ, Wagner RR.** 1980. Localization of membrane-associated proteins in vesicular stomatitis virus by use of hydrophobic membrane probes and cross-linking reagents. *Journal of virology* **36**:93-102.

17. **Le Mercier P, Jacob Y, Tordo N.** 1997. The complete Mokola virus genome sequence: structure of the RNA-dependent RNA polymerase. *The Journal of general virology* **78** (Pt 7):1571-1576.
18. **Marston DA, McElhinney LM, Johnson N, Muller T, Conzelmann KK, Tordo N, Fooks AR.** 2007. Comparative analysis of the full genome sequence of European bat lyssavirus type 1 and type 2 with other lyssaviruses and evidence for a conserved transcription termination and polyadenylation motif in the G-L 3' non-translated region. *The Journal of general virology* **88**:1302-1314.
19. **Krebs JW, Smith JS, Rupprecht CE, Childs JE.** 1997. Rabies surveillance in the United States during 1996. *Journal of the American Veterinary Medical Association* **211**:1525-1539.
20. **Gautret P, Parola P.** 2012. Rabies vaccination for international travelers. *Vaccine* **30**:126-133.
21. **Liu L.** 2014. *Fields Virology. Clinical infectious diseases : an official publication of the Infectious Diseases Society of America.*
22. **Ugolini G.** 2011. Rabies virus as a transneuronal tracer of neuronal connections. *Advances in virus research* **79**:165-202.
23. **Lafon M.** 2011. Evasive strategies in rabies virus infection. *Advances in virus research* **79**:33-53.
24. **Martinez L.** 2000. Global infectious disease surveillance. *International journal of infectious diseases : IJID : official publication of the International Society for Infectious Diseases* **4**:222-228.

25. **Bourhy H, Dautry-Varsat A, Hotez PJ, Salomon J.** 2010. Rabies, still neglected after 125 years of vaccination. *PLoS neglected tropical diseases* **4**:e839.
26. **Li J, Faber M, Dietzschold B, Hooper DC.** 2011. The role of toll-like receptors in the induction of immune responses during rabies virus infection. *Advances in virus research* **79**:115-126.
27. **Morimoto K, Patel M, Corisdeo S, Hooper DC, Fu ZF, Rupprecht CE, Koprowski H, Dietzschold B.** 1996. Characterization of a unique variant of bat rabies virus responsible for newly emerging human cases in North America. *Proceedings of the National Academy of Sciences of the United States of America* **93**:5653-5658.
28. **Both L, Banyard AC, van Dolleweerd C, Horton DL, Ma JK, Fooks AR.** 2012. Passive immunity in the prevention of rabies. *The Lancet infectious diseases* **12**:397-407.
29. **Jackson AC, Kammouni W, Zherebitskaya E, Fernyhough P.** 2010. Role of oxidative stress in rabies virus infection of adult mouse dorsal root ganglion neurons. *Journal of virology* **84**:4697-4705.
30. **Scott CA, Rossiter JP, Andrew RD, Jackson AC.** 2008. Structural abnormalities in neurons are sufficient to explain the clinical disease and fatal outcome of experimental rabies in yellow fluorescent protein-expressing transgenic mice. *Journal of virology* **82**:513-521.
31. **Galelli A, Baloul L, Lafon M.** 2000. Abortive rabies virus central nervous infection is controlled by T lymphocyte local recruitment and induction of apoptosis. *Journal of neurovirology* **6**:359-372.

32. **Jackson AC, Rossiter JP, Lafon M.** 2006. Expression of Toll-like receptor 3 in the human cerebellar cortex in rabies, herpes simplex encephalitis, and other neurological diseases. *Journal of neurovirology* **12**:229-234.
33. **Wang ZW, Sarmiento L, Wang Y, Li XQ, Dhingra V, Tseggai T, Jiang B, Fu ZF.** 2005. Attenuated rabies virus activates, while pathogenic rabies virus evades, the host innate immune responses in the central nervous system. *Journal of virology* **79**:12554-12565.
34. **Miyamoto K, Matsumoto S.** 1967. Comparative studies between pathogenesis of street and fixed rabies infection. *The Journal of experimental medicine* **125**:447-456.
35. **Murphy FA.** 1977. Rabies pathogenesis. *Archives of virology* **54**:279-297.
36. **Dorr J, Bechmann I, Waiczies S, Aktas O, Walczak H, Krammer PH, Nitsch R, Zipp F.** 2002. Lack of tumor necrosis factor-related apoptosis-inducing ligand but presence of its receptors in the human brain. *The Journal of neuroscience : the official journal of the Society for Neuroscience* **22**:RC209.
37. **Yan X, Prosniak M, Curtis MT, Weiss ML, Faber M, Dietzschold B, Fu ZF.** 2001. Silver-haired bat rabies virus variant does not induce apoptosis in the brain of experimentally infected mice. *Journal of neurovirology* **7**:518-527.
38. **Hooper DC, Phares TW, Fabis MJ, Roy A.** 2009. The production of antibody by invading B cells is required for the clearance of rabies virus from the central nervous system. *PLoS neglected tropical diseases* **3**:e535.
39. **Wiktor TJ, Macfarlan RI, Reagan KJ, Dietzschold B, Curtis PJ, Wunner WH, Kieny MP, Lathe R, Lecocq JP, Mackett M, et al.** 1984. Protection from rabies by a

- vaccinia virus recombinant containing the rabies virus glycoprotein gene. Proceedings of the National Academy of Sciences of the United States of America **81**:7194-7198.
40. **Zhang G, Wang H, Mahmood F, Fu ZF.** 2013. Rabies virus glycoprotein is an important determinant for the induction of innate immune responses and the pathogenic mechanisms. *Veterinary microbiology* **162**:601-613.
 41. **Lees CY, Briggs DJ, Wu X, Davis RD, Moore SM, Gordon C, Xiang Z, Ertl HC, Tang DC, Fu ZF.** 2002. Induction of protective immunity by topic application of a recombinant adenovirus expressing rabies virus glycoprotein. *Veterinary microbiology* **85**:295-303.
 42. **Wunner WH, Dietzschold B, Curtis PJ, Wiktor TJ.** 1983. Rabies subunit vaccines. *The Journal of general virology* **64 (Pt 8)**:1649-1656.
 43. **Janeway CA, Jr., Medzhitov R.** 2002. Innate immune recognition. *Annual review of immunology* **20**:197-216.
 44. **Faul EJ, Wanjalla CN, Suthar MS, Gale M, Wirblich C, Schnell MJ.** 2010. Rabies virus infection induces type I interferon production in an IPS-1 dependent manner while dendritic cell activation relies on IFNAR signaling. *PLoS pathogens* **6**:e1001016.
 45. **Kawai T, Akira S.** 2010. The role of pattern-recognition receptors in innate immunity: update on Toll-like receptors. *Nature immunology* **11**:373-384.
 46. **Yoneyama M, Fujita T.** 2010. Recognition of viral nucleic acids in innate immunity. *Reviews in medical virology* **20**:4-22.

47. **Ullas PT, Desai A, Madhusudana SN.** 2014. Immunogenicity and efficacy of a plasmid DNA rabies vaccine incorporating Myd88 as a genetic adjuvant. *Clinical and experimental vaccine research* **3**:202-211.
48. **Kebir H, Kreymborg K, Ifergan I, Dodelet-Devillers A, Cayrol R, Bernard M, Giuliani F, Arbour N, Becher B, Prat A.** 2007. Human TH17 lymphocytes promote blood-brain barrier disruption and central nervous system inflammation. *Nature medicine* **13**:1173-1175.
49. **Roy A, Hooper DC.** 2007. Lethal silver-haired bat rabies virus infection can be prevented by opening the blood-brain barrier. *Journal of virology* **81**:7993-7998.
50. **Vinet J, de Jong EK, Boddeke HW, Stanulovic V, Brouwer N, Granic I, Eisel UL, Liem RS, Biber K.** 2010. Expression of CXCL10 in cultured cortical neurons. *Journal of neurochemistry* **112**:703-714.
51. **Bhowmick S, Duseja R, Das S, Appaiahgiri MB, Vрати S, Basu A.** 2007. Induction of IP-10 (CXCL10) in astrocytes following Japanese encephalitis. *Neuroscience letters* **414**:45-50.
52. **Cheeran MC, Hu S, Sheng WS, Peterson PK, Lokensgard JR.** 2003. CXCL10 production from cytomegalovirus-stimulated microglia is regulated by both human and viral interleukin-10. *Journal of virology* **77**:4502-4515.
53. **Perkins ND.** 2007. Integrating cell-signalling pathways with NF-kappaB and IKK function. *Nature reviews. Molecular cell biology* **8**:49-62.

54. **Honda K, Taniguchi T.** 2006. IRFs: master regulators of signalling by Toll-like receptors and cytosolic pattern-recognition receptors. *Nature reviews. Immunology* **6**:644-658.
55. **Schindler C, Levy DE, Decker T.** 2007. JAK-STAT signaling: from interferons to cytokines. *The Journal of biological chemistry* **282**:20059-20063.
56. **Dufour JH, Dziejman M, Liu MT, Leung JH, Lane TE, Luster AD.** 2002. IFN-gamma-inducible protein 10 (IP-10; CXCL10)-deficient mice reveal a role for IP-10 in effector T cell generation and trafficking. *Journal of immunology* **168**:3195-3204.
57. **Liu M, Guo S, Hibbert JM, Jain V, Singh N, Wilson NO, Stiles JK.** 2011. CXCL10/IP-10 in infectious diseases pathogenesis and potential therapeutic implications. *Cytokine & growth factor reviews* **22**:121-130.
58. **Nakamichi K, Saiki M, Sawada M, Takayama-Ito M, Yamamuro Y, Morimoto K, Kurane I.** 2005. Rabies virus-induced activation of mitogen-activated protein kinase and NF-kappaB signaling pathways regulates expression of CXC and CC chemokine ligands in microglia. *Journal of virology* **79**:11801-11812.
59. **Kristensson K.** 2011. Microbes' roadmap to neurons. *Nature reviews. Neuroscience* **12**:345-357.
60. **Wu X, Gong X, Foley HD, Schnell MJ, Fu ZF.** 2002. Both viral transcription and replication are reduced when the rabies virus nucleoprotein is not phosphorylated. *Journal of virology* **76**:4153-4161.

61. **Menager P, Roux P, Megret F, Bourgeois JP, Le Sourd AM, Danckaert A, Lafage M, Prehaud C, Lafon M.** 2009. Toll-like receptor 3 (TLR3) plays a major role in the formation of rabies virus Negri Bodies. *PLoS pathogens* **5**:e1000315.
62. **Sarmiento L, Li XQ, Howerth E, Jackson AC, Fu ZF.** 2005. Glycoprotein-mediated induction of apoptosis limits the spread of attenuated rabies viruses in the central nervous system of mice. *Journal of neurovirology* **11**:571-581.
63. **Sarmiento L, Tseggai T, Dhingra V, Fu ZF.** 2006. Rabies virus-induced apoptosis involves caspase-dependent and caspase-independent pathways. *Virus research* **121**:144-151.
64. **Gratas C, Tohma Y, Barnas C, Taniere P, Hainaut P, Ohgaki H.** 1998. Up-regulation of Fas (APO-1/CD95) ligand and down-regulation of Fas expression in human esophageal cancer. *Cancer research* **58**:2057-2062.
65. **Rouas-Freiss N, Moreau P, Menier C, Carosella ED.** 2003. HLA-G in cancer: a way to turn off the immune system. *Seminars in cancer biology* **13**:325-336.
66. **Abbott NJ, Patabendige AA, Dolman DE, Yusof SR, Begley DJ.** 2010. Structure and function of the blood-brain barrier. *Neurobiology of disease* **37**:13-25.
67. **Hooper DC, Morimoto K, Bette M, Weihe E, Koprowski H, Dietzschold B.** 1998. Collaboration of antibody and inflammation in clearance of rabies virus from the central nervous system. *Journal of virology* **72**:3711-3719.
68. **Davson H.** 1976. Review lecture. The blood-brain barrier. *The Journal of physiology* **255**:1-28.

69. **Banks WA, Erickson MA.** 2010. The blood-brain barrier and immune function and dysfunction. *Neurobiology of disease* **37**:26-32.
70. **Jones AR, Shusta EV.** 2007. Blood-brain barrier transport of therapeutics via receptor-mediation. *Pharmaceutical research* **24**:1759-1771.
71. **Nieder Korn JY.** 2006. See no evil, hear no evil, do no evil: the lessons of immune privilege. *Nature immunology* **7**:354-359.
72. **Lampron A, Elali A, Rivest S.** 2013. Innate immunity in the CNS: redefining the relationship between the CNS and Its environment. *Neuron* **78**:214-232.
73. **Obermeier B, Daneman R, Ransohoff RM.** 2013. Development, maintenance and disruption of the blood-brain barrier. *Nature medicine* **19**:1584-1596.
74. **Woodland DL.** 2011. Viral infections: impact on chemokines and chemokine receptors. *Viral immunology* **24**:427-428.
75. **Abbott NJ, Ronnback L, Hansson E.** 2006. Astrocyte-endothelial interactions at the blood-brain barrier. *Nature reviews. Neuroscience* **7**:41-53.
76. **Bazzoni G, Dejana E.** 2004. Endothelial cell-to-cell junctions: molecular organization and role in vascular homeostasis. *Physiological reviews* **84**:869-901.
77. **Predescu SA, Predescu DN, Malik AB.** 2007. Molecular determinants of endothelial transcytosis and their role in endothelial permeability. *American journal of physiology. Lung cellular and molecular physiology* **293**:L823-842.
78. **Nitta T, Hata M, Gotoh S, Seo Y, Sasaki H, Hashimoto N, Furuse M, Tsukita S.** 2003. Size-selective loosening of the blood-brain barrier in claudin-5-deficient mice. *The Journal of cell biology* **161**:653-660.

79. **Bradbury MW, Lightman SL.** 1990. The blood-brain interface. *Eye* **4 (Pt 2):**249-254.
80. **Lehner C, Gehwolf R, Tempfer H, Krizbai I, Hennig B, Bauer HC, Bauer H.** 2011. Oxidative stress and blood-brain barrier dysfunction under particular consideration of matrix metalloproteinases. *Antioxidants & redox signaling* **15:**1305-1323.
81. **Hawkins BT, Davis TP.** 2005. The blood-brain barrier/neurovascular unit in health and disease. *Pharmacological reviews* **57:**173-185.
82. **Furuse M, Fujita K, Hiiragi T, Fujimoto K, Tsukita S.** 1998. Claudin-1 and -2: novel integral membrane proteins localizing at tight junctions with no sequence similarity to occludin. *The Journal of cell biology* **141:**1539-1550.
83. **Thurer RL, Popovsky MA.** 2011. Blood transfusion and the microcirculation. *Transfusion* **51:**2259.
84. **Engelhardt B, Sorokin L.** 2009. The blood-brain and the blood-cerebrospinal fluid barriers: function and dysfunction. *Seminars in immunopathology* **31:**497-511.
85. **Lai CH, Kuo KH.** 2005. The critical component to establish in vitro BBB model: Pericyte. *Brain research. Brain research reviews* **50:**258-265.
86. **Reese TS, Karnovsky MJ.** 1967. Fine structural localization of a blood-brain barrier to exogenous peroxidase. *The Journal of cell biology* **34:**207-217.
87. **Brightman MW, Reese TS.** 1969. Junctions between intimately apposed cell membranes in the vertebrate brain. *The Journal of cell biology* **40:**648-677.
88. **Sofroniew MV, Vinters HV.** 2010. Astrocytes: biology and pathology. *Acta neuropathologica* **119:**7-35.

89. **Nag S, Manias JL, Stewart DJ.** 2009. Pathology and new players in the pathogenesis of brain edema. *Acta neuropathologica* **118**:197-217.
90. **Argaw AT, Asp L, Zhang J, Navrazhina K, Pham T, Mariani JN, Mahase S, Dutta DJ, Seto J, Kramer EG, Ferrara N, Sofroniew MV, John GR.** 2012. Astrocyte-derived VEGF-A drives blood-brain barrier disruption in CNS inflammatory disease. *The Journal of clinical investigation* **122**:2454-2468.
91. **Huber JD, Egleton RD, Davis TP.** 2001. Molecular physiology and pathophysiology of tight junctions in the blood-brain barrier. *Trends in neurosciences* **24**:719-725.
92. **Jin R, Yang G, Li G.** 2010. Inflammatory mechanisms in ischemic stroke: role of inflammatory cells. *Journal of leukocyte biology* **87**:779-789.
93. **McAdams RM, Juul SE.** 2012. The role of cytokines and inflammatory cells in perinatal brain injury. *Neurology research international* **2012**:561494.
94. **Ballabh P, Braun A, Nedergaard M.** 2004. The blood-brain barrier: an overview: structure, regulation, and clinical implications. *Neurobiology of disease* **16**:1-13.
95. **Mathur A, Khanna N, Chaturvedi UC.** 1992. Breakdown of blood-brain barrier by virus-induced cytokine during Japanese encephalitis virus infection. *International journal of experimental pathology* **73**:603-611.
96. **Spindler KR, Hsu TH.** 2012. Viral disruption of the blood-brain barrier. *Trends in microbiology* **20**:282-290.
97. **Sellner J, Simon F, Meyding-Lamade U, Leib SL.** 2006. Herpes-simplex virus encephalitis is characterized by an early MMP-9 increase and collagen type IV degradation. *Brain research* **1125**:155-162.

98. **Zougbede S, Miller F, Ravassard P, Rebollo A, Ciceron L, Couraud PO, Mazier D, Moreno A.** 2011. Metabolic acidosis induced by Plasmodium falciparum intraerythrocytic stages alters blood-brain barrier integrity. *Journal of cerebral blood flow and metabolism : official journal of the International Society of Cerebral Blood Flow and Metabolism* **31**:514-526.
99. **Kang SS, McGavern DB.** 2010. Microbial induction of vascular pathology in the CNS. *Journal of neuroimmune pharmacology : the official journal of the Society on NeuroImmune Pharmacology* **5**:370-386.
100. **Prato M, D'Alessandro S, Van den Steen PE, Opdenakker G, Arese P, Taramelli D, Basilico N.** 2011. Natural haemozoin modulates matrix metalloproteinases and induces morphological changes in human microvascular endothelium. *Cellular microbiology* **13**:1275-1285.
101. **Lacerda-Queiroz N, Lima OC, Carneiro CM, Vilela MC, Teixeira AL, Teixeira-Carvalho A, Araujo MS, Martins-Filho OA, Braga EM, Carvalho-Tavares J.** 2011. Plasmodium berghei NK65 induces cerebral leukocyte recruitment in vivo: an intravital microscopic study. *Acta tropica* **120**:31-39.
102. **Gralinski LE, Ashley SL, Dixon SD, Spindler KR.** 2009. Mouse adenovirus type 1-induced breakdown of the blood-brain barrier. *Journal of virology* **83**:9398-9410.
103. **Guida JD, Fejer G, Pirofski LA, Brosnan CF, Horwitz MS.** 1995. Mouse adenovirus type 1 causes a fatal hemorrhagic encephalomyelitis in adult C57BL/6 but not BALB/c mice. *Journal of virology* **69**:7674-7681.

104. **Kring SC, King CS, Spindler KR.** 1995. Susceptibility and signs associated with mouse adenovirus type 1 infection of adult outbred Swiss mice. *Journal of virology* **69**:8084-8088.
105. **Kajon AE, Brown CC, Spindler KR.** 1998. Distribution of mouse adenovirus type 1 in intraperitoneally and intranasally infected adult outbred mice. *Journal of virology* **72**:1219-1223.
106. **Verma S, Kumar M, Gurjav U, Lum S, Nerurkar VR.** 2010. Reversal of West Nile virus-induced blood-brain barrier disruption and tight junction proteins degradation by matrix metalloproteinases inhibitor. *Virology* **397**:130-138.
107. **Wang T, Town T, Alexopoulou L, Anderson JF, Fikrig E, Flavell RA.** 2004. Toll-like receptor 3 mediates West Nile virus entry into the brain causing lethal encephalitis. *Nature medicine* **10**:1366-1373.
108. **Daffis S, Samuel MA, Suthar MS, Gale M, Jr., Diamond MS.** 2008. Toll-like receptor 3 has a protective role against West Nile virus infection. *Journal of virology* **82**:10349-10358.
109. **Husmann KL, Fredericksen BL.** 2014. Differential induction of CCL5 by pathogenic and non-pathogenic strains of West Nile virus in brain endothelial cells and astrocytes. *The Journal of general virology* **95**:862-867.
110. **Klein RS, Lin E, Zhang B, Luster AD, Tollett J, Samuel MA, Engle M, Diamond MS.** 2005. Neuronal CXCL10 directs CD8⁺ T-cell recruitment and control of West Nile virus encephalitis. *Journal of virology* **79**:11457-11466.

111. **Liu LP, Liang HF, Chen XP, Zhang WG, Yang SL, Xu T, Ren L.** 2010. The role of NF-kappaB in Hepatitis b virus X protein-mediated upregulation of VEGF and MMPs. *Cancer investigation* **28**:443-451.
112. **Avraham HK, Jiang S, Lee TH, Prakash O, Avraham S.** 2004. HIV-1 Tat-mediated effects on focal adhesion assembly and permeability in brain microvascular endothelial cells. *Journal of immunology* **173**:6228-6233.
113. **Pu H, Hayashi K, Andras IE, Eum SY, Hennig B, Toborek M.** 2007. Limited role of COX-2 in HIV Tat-induced alterations of tight junction protein expression and disruption of the blood-brain barrier. *Brain research* **1184**:333-344.
114. **Louboutin JP, Agrawal L, Reyes BA, Van Bockstaele EJ, Strayer DS.** 2010. HIV-1 gp120-induced injury to the blood-brain barrier: role of metalloproteinases 2 and 9 and relationship to oxidative stress. *Journal of neuropathology and experimental neurology* **69**:801-816.
115. **Sporer B, Koedel U, Paul R, Kohleisen B, Erfle V, Fontana A, Pfister HW.** 2000. Human immunodeficiency virus type-1 Nef protein induces blood-brain barrier disruption in the rat: role of matrix metalloproteinase-9. *Journal of neuroimmunology* **102**:125-130.
116. **Kuang Y, Lackay SN, Zhao L, Fu ZF.** 2009. Role of chemokines in the enhancement of BBB permeability and inflammatory infiltration after rabies virus infection. *Virus research* **144**:18-26.
117. **Eugenin EA, Osiecki K, Lopez L, Goldstein H, Calderon TM, Berman JW.** 2006. CCL2/monocyte chemoattractant protein-1 mediates enhanced transmigration of human

- immunodeficiency virus (HIV)-infected leukocytes across the blood-brain barrier: a potential mechanism of HIV-CNS invasion and NeuroAIDS. *The Journal of neuroscience : the official journal of the Society for Neuroscience* **26**:1098-1106.
118. **Stamatovic SM, Keep RF, Kunkel SL, Andjelkovic AV.** 2003. Potential role of MCP-1 in endothelial cell tight junction 'opening': signaling via Rho and Rho kinase. *Journal of cell science* **116**:4615-4628.
119. **Dimitrijevic OB, Stamatovic SM, Keep RF, Andjelkovic AV.** 2006. Effects of the chemokine CCL2 on blood-brain barrier permeability during ischemia-reperfusion injury. *Journal of cerebral blood flow and metabolism : official journal of the International Society of Cerebral Blood Flow and Metabolism* **26**:797-810.
120. **Ifergan I, Kebir H, Bernard M, Wosik K, Dodelet-Devillers A, Cayrol R, Arbour N, Prat A.** 2008. The blood-brain barrier induces differentiation of migrating monocytes into Th17-polarizing dendritic cells. *Brain : a journal of neurology* **131**:785-799.
121. **Subileau EA, Rezaie P, Davies HA, Colyer FM, Greenwood J, Male DK, Romero IA.** 2009. Expression of chemokines and their receptors by human brain endothelium: implications for multiple sclerosis. *Journal of neuropathology and experimental neurology* **68**:227-240.
122. **Jackson AC, Kammouni W, Fernyhough P.** 2011. Role of oxidative stress in rabies virus infection. *Advances in virus research* **79**:127-138.
123. **Argaw AT, Gurfein BT, Zhang Y, Zameer A, John GR.** 2009. VEGF-mediated disruption of endothelial CLN-5 promotes blood-brain barrier breakdown. *Proceedings of the National Academy of Sciences of the United States of America* **106**:1977-1982.

124. **Zhao L, Toriumi H, Kuang Y, Chen H, Fu ZF.** 2009. The roles of chemokines in rabies virus infection: overexpression may not always be beneficial. *Journal of virology* **83**:11808-11818.
125. **Moser B, Loetscher P.** 2001. Lymphocyte traffic control by chemokines. *Nature immunology* **2**:123-128.
126. **Martin-Fontecha A, Thomsen LL, Brett S, Gerard C, Lipp M, Lanzavecchia A, Sallusto F.** 2004. Induced recruitment of NK cells to lymph nodes provides IFN-gamma for T(H)1 priming. *Nature immunology* **5**:1260-1265.
127. **Tsunoda I, Lane TE, Blackett J, Fujinami RS.** 2004. Distinct roles for IP-10/CXCL10 in three animal models, Theiler's virus infection, EAE, and MHV infection, for multiple sclerosis: implication of differing roles for IP-10. *Multiple sclerosis* **10**:26-34.
128. **Stiles LN, Hosking MP, Edwards RA, Strieter RM, Lane TE.** 2006. Differential roles for CXCR3 in CD4+ and CD8+ T cell trafficking following viral infection of the CNS. *European journal of immunology* **36**:613-622.
129. **Narumi S, Kaburaki T, Yoneyama H, Iwamura H, Kobayashi Y, Matsushima K.** 2002. Neutralization of IFN-inducible protein 10/CXCL10 exacerbates experimental autoimmune encephalomyelitis. *European journal of immunology* **32**:1784-1791.
130. **Liu L, Huang D, Matsui M, He TT, Hu T, Demartino J, Lu B, Gerard C, Ransohoff RM.** 2006. Severe disease, unaltered leukocyte migration, and reduced IFN-gamma production in CXCR3^{-/-} mice with experimental autoimmune encephalomyelitis. *Journal of immunology* **176**:4399-4409.

131. **Chai Q, He WQ, Zhou M, Lu H, Fu ZF.** 2014. Enhancement of blood-brain barrier permeability and reduction of tight junction protein expression are modulated by chemokines/cytokines induced by rabies virus infection. *Journal of virology* **88**:4698-4710.

CHAPTER 3

ENHANCEMENT OF BLOOD-BRAIN BARRIER PERMEABILITY AND REDUCTION OF TIGHT JUNCTION PROTEIN EXPRESSION ARE MODULATED BY CHEMOKINES/CYTOKINES INDUCED BY RABIES VIRUS INFECTION

Qingqing Chai, Wen Q. He, Ming Zhou, Huijun Lu, Zhen F. Fu

Journal of Virology. JVI.03149-13.

Reprinted there with the permission of the publisher

I. Abstract

Previous studies have shown that infection with laboratory-attenuated, but not wild type (wt), rabies virus (RABV) induces the expression of innate immune genes, infiltration of inflammatory cells into the CNS, and enhancement of Blood-brain Barrier (BBB) permeability. Enhancement of BBB permeability has been demonstrated to be an important factor for host survival since it allows immune effectors to enter into the CNS to clear RABV. To probe the mechanism by which RABV infection enhances BBB permeability, the expression of tight junction (TJ) proteins in the CNS was investigated following intracranial inoculation with laboratory-attenuated or wt RABV. BBB permeability was significantly enhanced in mice infected with laboratory-attenuated, but not wt, RABV. The expression levels of TJ proteins (claudin-5, occludin, and Zonula Occludens-1) were decreased in mice infected with laboratory-attenuated, but not wt, RABV, suggesting that enhancement of BBB permeability is associated with reduction of TJ protein expression in RABV infection. RABV neither infected the brain microvascular endothelial cells (BMECs) nor modulated the expression of TJ proteins in BMECs. However, brain extracts prepared from mice infected with laboratory-attenuated, but not wt, RABV reduced TJ protein expressions in BMECs. It was found that brain extracts from mice infected with laboratory-attenuated RABV contained significantly higher levels of inflammatory chemokines/cytokines than those from mice infected with wt RABV. Pathway analysis indicates that IFN- γ is located in the center of the cytokine network in RABV-infected mouse brain and neutralization of IFN- γ ameliorated both disruption of BBB permeability *in vivo*

and down-regulation of TJ protein expression *in vitro*. These findings indicate that enhancement of BBB permeability and reduction of TJ protein expressions are not due to RABV infection per se, but due to virus-induced inflammatory chemokines/cytokines.

Key Words: Rabies virus, Blood-brain Barrier (BBB), Tight Junction proteins, ZO-1, claudin-5, occludin, chemokines, cytokines

II. Introduction

Rabies virus (RABV) is a negative-stranded RNA virus belonging to the genus *Lyssavirus* within the family *Rhabdoviridae* (1-3). RABV causes fatal encephalomyelitis resulting in more than 55,000 human deaths annually (2, 4). RABV enters neurons in the periphery at the wound site and then travels to the central nervous system (CNS) via sensory and motor neurons. Despite of dramatic clinical symptoms and outcome, surprisingly little tissue damage or neuronal pathology was observed in brains of rabid patients (5). In the mouse model, inflammation is mild after infection with wild-type (wt) RABV (6). However, extensive inflammation, apoptosis, and expression of innate immune genes were found in the CNS of mice infected with laboratory-attenuated RABV (7-12). Recently, it has been found that Blood-brain Barrier (BBB) permeability is enhanced in mice infected with laboratory-attenuated, but not wt, RABV (10, 13). Enhancement of BBB permeability is important in RABV attenuation by allowing immune effectors enter into the CNS to clear RABV (6, 10, 14). Therefore,

enhancement of BBB permeability by using disease model (i.e. EAE, experimental autoimmune encephalomyelitis) (15, 16) as well as by administering laboratory-attenuated RABV, recombinant RABVs expressing three copies of the glycoprotein (G) (17) or immune stimulating agents (18) resulted in clearing wt RABV from the CNS and preventing the development of rabies in mice.

BBB is non-fenestrated to large molecules or xenobiotics, thus providing protection against the invasion of macromolecules and microorganisms into the CNS (19). BBB is composed of endothelial cells (ECs), pericytes, and astrocytes (20). Alteration of BBB permeability is observed both in bacterial and viral infections. One of the key mechanisms of BBB breakdown is the damage of tight junction (TJ) in the brain microvascular ECs (BMEC) (19). TJ complex is composed of both transmembrane TJ proteins (occludin and claudins) and cytosolic TJ proteins (Zonula Occludens-1, ZO-1) that link transmembrane TJ proteins to actin cytoskeleton (21-23). Many viral infections such as infection of human immunodeficiency virus (HIV), Japanese encephalitis virus (JEV), mouse adenovirus type-1 (MAV-1) trigger changes in BBB permeability (24-26). Some of the viruses (for instance MAV-1) enhance BBB permeability by direct disruption of TJ complex in primary ECs (26), while others (for example HIV) disrupt the TJ complex and enhance BBB permeability via inducing the expression of chemokines (particularly CCL2) in the CNS (24). In the EAE model, disruption of BBB is associated with infiltration of T-helper cells (27) and production of IL-17A. IL-17A in T-helper 17 cell-signaling pathways has been demonstrated to induce down-regulation of TJ proteins and influx of immune cells in C57BL/6 mice (28, 29). In the present study, the mechanism by which RABVs enhance

BBB permeability is investigated and it is found that enhancement of BBB permeability and reduction of TJ protein expression are not associated with direct RABV infection, but rather are associated with the expression of chemokines/cytokines after infection with laboratory-attenuated RABV.

III. Materials and Methods

Cells, viruses, antibodies and mice. Mouse brain microvascular EC (bEnd.3) was obtained from American Type Culture Collection (ATCC, Manassas, VA) and maintained in Dulbecco's Modified Eagle's Medium (DMEM) supplemented with fetal bovine serum (FBS) (ATCC). Human brain microvascular EC line (hBMEC) was obtained from Dr. Jason Zastre in the College of Pharmacy, University of Georgia. Mouse neuroblastoma (mNA) cells were maintained in RPMI 1640 medium (Mediatech, Herndon, VA) supplemented with 10% FBS. DRV-Mexico is a wt virus originated from a Mexican dog and propagated in suckling mouse brain (30). CVS-B2c is a laboratory-attenuated RABV by passaging the challenge virus standard (CVS-24) in baby hamster kidney (BHK21) cells (31). Recombinant virus HEP-CXCL10 (rHEP-CXCL10) was constructed previously in our laboratory (7). Fluorescein isothiocyanate (FITC)-conjugated anti-RABV-nucleoprotein antibody was obtained from FujiRebio (Malvern, PA). Rabbit polyclonal anti-occludin and anti-actin antibodies were obtained from Santa Cruz Biotechnology (Santa Cruz, CA). Anti-IFN- γ Antibody (XMG1.2) and mouse IgG1 isotype control antibody were purchased from Thermo Scientific (Suwanee, GA). Rabbit polyclonal anti-

claudin-5 antibody, biotinylated goat anti-rabbit antibody, and Alexa-Fluor 488-conjugated goat anti-rabbit antibody were purchased from Invitrogen (Grand Island, NY). Mouse monoclonal anti-ZO-1 and rabbit polyclonal anti-CD3 antibodies were obtained from Sigma (St. Louis, MO) and Abcam (Cambridge, MA), respectively. Female ICR mice (4-6 weeks old) were purchased from Harlan and housed in the animal facility in the College of Veterinary Medicine, University of Georgia. All animal experiments were carried out under the Institutional Animal Care and Use Committee-approved protocols (animal welfare assurance No. A3058-01).

Measurement of BBB permeability. BBB permeability was determined by measuring Sodium Fluorescein (NaF) uptake as previously described (32). Briefly, NaF was used as the tracer; 100 μ l of 100 mg/mL of NaF was injected to each mouse through the tail vein. Peripheral blood was collected after circulation for 10 min and phosphate-buffered saline (PBS)-perfused brains were then harvested. Serum recovered was mixed with equal volume of 10% trichloroacetic acid (TCA) and then centrifuged for 10 min. The supernatant was collected after centrifugation and made up to 150 μ l by mixing with 5M NaOH and 7.5% TCA. Homogenized brain samples in cold 7.5% TCA were centrifuged for 10 min at 10,000 \times g to remove debris. The supernatant was made up to 150 μ l by adding 5M NaOH. The fluorescence of serum and brain homogenate samples was measured using a spectrophotometer (BioTek Instruments, VT) with excitation at 485 nm and emission at 530 nm. NaF taken up into brain tissues is expressed as the micrograms of fluorescence per mg of cerebrum or cerebellum divided by the micrograms of fluorescence per μ l of serum to normalize the uptake amounts of tracer from peripheral blood at

the time of brain tissue collection (32, 33). Data are expressed as a fold change in the amount of tracer in tissues by comparison with the values obtained for tissues from negative control.

Histopathology, immunohistochemistry (IHC), and quantitative Western blotting (WB) analysis. For histopathology and IHC, infected mice were anesthetized with ketamine-xylazine (0.1 ml/10 g body weight) and perfused with PBS followed by 10% neutral buffered formalin as described previously (12, 34). Three independent samples of mice brains were harvested from each group. Brain tissues were removed and paraffin-embedded for coronal sections (4 μ m). The sections were stained with hematoxylin and eosin (HE) for histopathology. For IHC, the sections were deparaffinized and rehydrated in xylene and ethanol. Endogenous peroxidase was quenched by incubation in 5% hydrogen peroxide and antigen retrieval was performed in citrate buffer (Fisher Scientific, NH). Sections were then blocked with goat serum and incubated with primary antibodies overnight at 4°C and then biotinylated secondary antibodies. The avidin-biotin-peroxidase complex (VectaStain Standard ABC kit, Vector Laboratories, Burlingame, CA) was used to localize the biotinylated antibody. Diaminobenzidine (DAB, Vector Laboratories) was utilized for color development. Negative control was performed by substituting primary antibodies with PBS. For antigen quantification, sections were photographed and analyzed using Olympus BX41 Microscope (Tokyo, Japan). Integrated Optical Density (IOD) of DAB signals was determined by Image-pro Plus 4.5 software (Media Cybernetics, Bethesda, MD).

For WB, three independent samples of mouse brains from each group were collected, homogenized and prepared as 10% (w/v) suspension in DMEM. After centrifugation, the

supernatants were collected and stored in -80°C . The brain extracts or cell lysates were subjected to 8%-16% sodium dodecyl sulfate polyacrylamide gel electrophoresis (SDS-PAGE) (Thermo Scientific, Rockford, IL). Separated proteins were electroblotted onto nitrocellulose membranes and incubated with primary antibodies overnight. After extensive washing with PBS, the blots were incubated with secondary antibodies. Proteins were detected by SuperSignal West Pico chemiluminescence (Thermo Scientific). Band signals corresponding to immunoreactive proteins were captured and chemiluminescence intensities were analyzed using ChemiDoc 4000 MP documentation System (Biorad, CA).

Infection of BMEC with RABV. Monolayer of bEnd.3 or hBMEC in six-well plates was co-cultured with RABV at a multiplicity of infection (MOI) of 1. Viruses were seeded and incubated with cells for 1 h at 37°C and then cells were washed three times with PBS (35). Plates were refilled with fresh medium and incubated at 34°C for 120 h. Supernatant was harvested for virus titration and the cells were fixed with pre-cold acetone for viral antigen detection. mRNA cells infected with RABVs were included as positive control. Virus titer was determined by direct fluorescent-antibody assay (dFA) as described (36). Acetone-fixed cells were stained with FITC-conjugated anti-RABV N antibody. Antigen-positive foci were captured under a fluorescent microscope (Zeiss, Germany). All experiments were carried out in quadruplicate.

Quantitative RT-PCR. Monolayer of bEnd.3 or hBMEC in six-well plates was co-cultured with RABV at a multiplicity of infection (MOI) of 1. Plates were incubated at 37°C , cells and culture supernatants were harvested at 24, 48h, and 120h. RNA was extracted from MBECs infected with RABV using the RNAeasy Mini Kit (Qiagen, Germany). Total RNA was

quantified using NanoDrop ND-2000 1-position spectrophotometer (UX-83061-00, DE) and reverse transcribed into complementary DNA using the SuperScript III first-strand synthesis system for RT-PCR (Invitrogen, NY) according to the manufacturer's instructions. Real-time quantitative PCR was performed using the Brilliant II SYBR green QRT-PCR master mix kit (Agilent Technologies, CA). PCR was performed in 20 ul with 2ul of the reverse transcribed product corresponding to 500 ng of total RNA, 12.5 ul of the master mix and 0.5 ul of dye with the following temperature profile: 95°C for 10 min and 40 cycles of 95°C for 30 s and 55°C for 1 min. For RABV-N gene detection, the following set of primers was used: forward, 5'GGAAAAGGGACATTTGAAAGAA3', reverse, 5' AGTCCTCGTCATCAGAGTTGAC3'. Analysis of gene expression was performed in an Mx 3000P apparatus (Stratagene, La Jolla, CA).

Immunofluorescence and confocal microscopy. RABV was seeded on monolayer of bEnd.3 at an MOI of 1 for 24 h at 37°C on coverslips and cells were fixed with 4% paraformaldehyde and stained with antibodies to TJ proteins. In addition, 10% (wt/vol) suspension of brain extract was prepared by homogenizing brain tissues in DMEM containing Complete Proteinase Inhibitor Cocktail (Roche, Germany). Brain homogenates were centrifuged to remove debris, and supernatants were harvested and seeded onto monolayers of bEnd.3 cells for 24 h. Cells were fixed and permeabilized with 0.2% Triton X-100. The expression of TJ protein was detected using primary anti-occludin or anti-claudin-5 antibodies. After washing, cells were incubated with Alexa-Fluor 488-conjugated goat anti-rabbit secondary antibody for 1 h at RT. Samples were mounted using Prolong Gold antifade reagent with DAPI (4', 6'-di-

amidino-2-phenylindole) (Invitrogen, NY) and visualized with Nikon A1 Confocal Laser Microscope System equipped with NIS-Elements 4.13 imaging software (Melville, NY). The images recorded were quantified using NIH's Fiji (downloaded from pacific.mpi-cbg.de/wiki/index.php/fiji), a distribution package of ImageJ, The mean fluorescence intensity (MFI) was calculated using region of interest (ROI), which was drawn around an entire cell so that it always included the membrane. Three independent experiments were carried out for each condition. Background staining was accounted for by using three negatively stained regions per cell, which were subtracted from the total mean fluorescence.

Determination of cytokine expression in brain extracts. Extracts from homogenized brains were analyzed simultaneously for concentrations of 30 mouse chemokines/cytokines using the Milliplex MAP 30-plex premixed mouse cytokine/chemokine magnetic bead panel (Millipore, Billerica, MA) (37) according to the manufacturer's instructions. The 30 cytokines and chemokines analyzed included CSF1, CSF3, VEGF, LIF, CSF2, TNF- α , IL-1 α , IL-2, IL-3, IL-4, IL-5, IL-6, IL-7, IL-10, IL-12p40, IL-12p70, IL-13, IL-15, IL-17, IFNG, CCL2, CCL3, CCL4, CCL5, CCL11, CXCL1, CXCL2, CXCL9, CXCL10, and CXCL5. Premixed magnetic beads conjugated to antibodies for all 30 analytes were mixed with equal volume of brain extracts in 96-well plates. Plates were protected from light and incubated on an orbital shaker overnight at 4°C, and magnetic beads were washed with 200 μ L of wash buffer for three times. Then detection antibodies were added to each well and incubated at RT for 1 h. Streptavidin-phycoerythrin was added to each well and incubated at RT for 30 min. The magnetic beads were resuspended in sheath fluid and plate was assayed on MAGPIX® with xPONENT software.

Median Fluorescent Intensity data were analyzed using a 5-parameter logistic method for calculating cytokine/chemokine concentrations in brain homogenates.

Ingenuity Pathway Analysis. The differentially expressed gene list (Luminex) was loaded into Ingenuity Pathway Analysis (IPA) 5.0 software (<http://www.ingenuity.com>) to perform biological network and functional analyses. IPA is a web-based software application containing most literature knowledge of biologic interactions between gene products. When using the IPA software, the networks obtained describe functional relationships between gene products based on known interactions in the literature. The IPA tool then associates these networks with known biologic functions and canonical pathways. Canonical pathway analysis identifies the pathways from the IPA library that are most significant to the data set.

IFN- γ neutralization in vivo. RABV-infected mice were treated with 100 μ g of anti-IFN- γ or isotype control antibody in 100 μ l sterile PBS via the intraperitoneal route (i.p.) at 0, 2, and 4 days p.i. Sham-infected mice received 100 μ l of sterile PBS as the control. Three mice were included in each group. At six days p.i., BBB permeability was determined by measuring NaF uptake as previously described (32). Data are expressed as the fold change in the amount of tracer in tissues by comparison with the values obtained for tissues from negative controls.

Statistical analysis. Data are expressed as mean \pm SEM and evaluation of the significance of differences between groups was performed by using student's t-test or using one-way analysis of variance (ANOVA) with Tukey's post hoc tests. $P < 0.05$ was considered as statistically significant in all studies. Graphs were plotted and analyzed using Graphpad Prism 5.0 (La Jolla, CA).

IV. Results

Laboratory-attenuated RABV enhanced more BBB permeability than wt RABV.

Previous studies demonstrated that laboratory-attenuated CVS-B2c, but not wt DRV-Mexico, enhanced BBB permeability via intramuscular infection (6). To investigate if intracranial infection with each of the viruses (DRV-Mexico or CVS-B2c) induces similar changes in BBB permeability, leakage of NaF from peripheral circulation into the CNS was measured in the cerebrum or cerebellum of mice infected with each of the viruses. At day 6 p.i., the BBB was found to be significantly more permeable in the cerebrum of mice infected with 10 MICLD₅₀ (mouse intracerebral lethal dose 50%) CVS-B2c (more than 3 fold increase in NaF uptake) than those infected with DRV-Mexico (almost no change) even when 10 times more virus was used (100LD₅₀DRV-Mexico) (Fig. 3.1A). No significant difference was detected in BBB permeability change in the cerebellum at this time point. By day 9 p.i., BBB permeability in the cerebrum of mice infected with CVS-B2c continued to be enhanced (more than 4 fold increase in NaF uptake). The most significant BBB permeability enhancement was observed in the cerebellum of mice infected with 10LD₅₀CVS-B2c (more than 7 fold increase in NaF uptake) at day 9 p.i. (Fig. 3.1A). At this time point, the NaF uptake had 2-4 fold increase in the cerebellum of mice infected with DRV-Mexico, indicating that BBB permeability was not increased until the end of the disease process in mice infected with wt RABV (at day 9 p.i. almost all animals developed severe diseases and reached the humane point for euthanasia). Overall, BBB permeability in the

CNS was significantly more enhanced in mice infected with CVS-B2c than in those infected with DRV-Mexico ($p<0.05$).

Laboratory-attenuated RABV induced more infiltration of inflammatory cells into the CNS than wt RABV. To investigate the effects of BBB permeability enhancement on cell infiltration, mice were infected with each of the RABVs and the brains were harvested and stained with HE. Perivascular cuffing and neuronal degeneration were observed in the brains of mice infected with CVS-B2c at days 6 and 9 p.i., while there were only few cells accumulated in the perivascular space of mice infected with DRV-Mexico at 6 days p.i. (Fig. 3.1B). It has been demonstrated that CD4⁺ T cells are required to enhance BBB permeability in the RABV infection (32). To quantify the infiltrating T cells, CD3 was chosen as the T cell marker. Brain sections were stained with anti-CD3 antibodies and the numbers of CD3⁺ T cells were estimated. As shown in Fig. 3.1B, CD3⁺ T cells were seen surrounding blood vessels of mice inoculated with low dose or invaded the parenchyma in mice infected with high dose of CVS-B2c at day 6 p.i., but only mice infected with high dose of CVS-B2c showed significantly more CD3⁺ T cells compared with control (Fig. 3.1C). Almost no CD3⁺ T cells were seen in mice infected with DRV-Mexico at this time point. By day 9 p.i., significantly more CD3⁺ T cells was seen surrounding blood vessels and in the parenchyma of mice infected with both low and high doses of CVS-B2c compared with control (Fig. 3.1B). Few CD3⁺ T cells were observed in mice infected with low dose while more CD3⁺ T cells surrounding the vessels in mice infected with high dose of DRV-Mexico (Fig. 3.1B and 3.1C). Overall, significantly more infiltrated T cells were detected in the CNS of mice infected with CVS-B2c than with DRV-Mexico ($p<0.01$) (Fig. 3.1C).

Laboratory-attenuated RABV reduced more TJ protein expression in the CNS than wt RABV. To provide insight into the mechanisms by which laboratory-attenuated RABV enhances BBB permeability, the expression levels of TJ proteins (claudin-5, occludin, and ZO-1) were assessed in the brains of mice infected with CVS-B2c or DRV-Mexico by IHC and quantitative WB using antibodies to each of the TJ proteins. The immune reactivities of transmembrane TJ proteins claudin-5 and occludin in the brains of mice infected with DRV-Mexico were similar to those seen in the brains of sham-infected mice, while staining of occludin and claudin-5 was partially lost in the brains of mice infected with CVS-B2c at day 6 p.i. (Fig. 3.2A). Integrated Optical Densities (IODs) of both occludin and claudin-5 staining were significantly decreased in the brains of mice infected with CVS-B2c when compared to those in the brains of sham-infected mice or mice infected with DRV-Mexico at day 6 p.i. The reductions were even more dramatic in mice infected with CVS-B2c by day 9 p.i. (Fig. 3.2B). Likewise, the pattern of cytoplasmic TJ protein ZO-1 in the brains of mice infected with DRV-Mexico was similar to that in sham-infected mice at day 6 p.i., while the expression level of ZO-1 in mice infected with CVS-B2c was significantly diminished at day 6 p.i. ($p < 0.01$). Overall, expression levels of ZO-1, occludin and claudin-5 were reduced to 3.04%, 5.47% and 6.34% respectively in mice infected with CVS-B2c when compared to those in sham-infected mice at day 9 p.i. (Fig. 3.2B). WB confirmed the observation by IHC (Fig. 3.2C). The expression levels of TJ proteins were significantly lower in mice infected with CVS-B2c (particularly in mice infected with high dose at day 9 p.i.) than those in sham-infected mice or in mice infected with DRV-Mexico (Fig. 3.2D). By day 9 p.i., the expression of TJ proteins in mice infected with DRV-Mexico was slightly decreased, corresponding to the increased BBB permeability, particularly in those

infected with the higher dose of DRV-Mexico. These results indicate that the TJ complex is broken down in mice infected with laboratory-attenuated CVS-B2c.

Neither laboratory-attenuated nor wt RABV infected BMECs or affected the expressions of TJ proteins in BMECs. To determine whether laboratory-attenuated RABV infection causes direct damage to BMECs, laboratory-attenuated CVS-B2c or wt DRV-Mexico was inoculated onto human or mouse BMECs at an MOI of 1. mNA cells were infected with each of the viruses as positive controls. As shown in Fig. 3.3A, both RABVs productively replicated in mNA cells as demonstrated by viral antigen staining. No RABV antigen was detectable in the monolayers of hBMEC or bEnd.3 cells, indicating that neither DRV-Mexico nor CVS-B2c infected BMECs (Fig. 3.3A). Phase contrast showed that bEnd.3 cells and hBMECs were viable at this time. Virus infection was further detected by quantitative RT-PCR (qRT-PCR) (Fig. 3.3B). Viral RNA decreased in the culture by 24 and 48 h p.i. and became non-detectable by 120 h p.i. The expression levels of TJ proteins were also investigated in RABV-infected BMECs. No significant difference in the expression level of occludin or claudin-5 was found between sham-treated bEnd.3 cells and cells inoculated with either RABV (Fig. 3.3C). Since previous studies showed that infection with rRABV expressing CXCL10 (rHEP-CXCL10) enhanced the BBB permeability (7), the supernatant from mNA cells infected with rHEP-CXCL10 (containing high concentration of CXCL10) was inoculated with bEnd.3 cells for 24 h. As shown in Fig. 3.3C, the expression level of occludin or claudin-5 decreased to undetectable level. These results suggest that RABV does not infect BMECs and the loss of TJ protein expression is not due to direct RABV infection.

TJ protein expression was altered by brain extracts prepared from mice infected with laboratory-attenuated. Since direct RABV inoculation does not alter the expression of TJ proteins in BMECs, brain extracts prepared from mice infected with either RABV were co-cultured with bEnd.3 cells and the expression levels of TJ proteins were assessed by confocal microscopy. As shown in Fig. 3.4A, strong peripheral patterns of claudin-5 and occludin were observed in bEnd.3 cells treated with brain extracts prepared from sham-infected mice. Similar patterns were also observed in cells treated with brain extracts from mice infected with DRV-Mexico at day 6 p.i., although the expression levels of occludin and claudin-5 were reduced at the periphery of bEnd.3 cells treated with brain extracts from mice infected with 100 LD50DRV-Mexico at day 9 p.i. (Fig. 3.4B). In contrast, expression of TJ proteins was significantly decreased in bEnd.3 cells treated with brain extracts prepared from mice infected with CVS-B2c at both at day 6 and 9 p.i. (Fig. 3.4B). These observations were confirmed by quantitative Western blotting (Fig. 3.4C). The expressions of TJ proteins (occludin and claudin-5) diminished almost completely in bEnd.3 cells when treated with brain extracts prepared from mice infected with CVS-B2c at day 9 p.i. (Fig. 3.4D). Overall, these results indicate that the expression of TJ protein is affected more by molecules in the brain extracts from mice infected with laboratory-attenuated RABV than those in the brain extracts from mice infected with wt RABV.

Cytokine profiling showed significantly more elevated chemokines/cytokines in the brain extracts of mice infected with laboratory-attenuated RABV than wt RABV. To analyze expression levels of chemokines/cytokines in the brain extracts that might be responsible for the reduction of TJ protein expression in BMECs, cytokine profiling was performed using Milliplex MAP 30-plex premixed mouse cytokine/chemokine magnetic bead panel. This panel

was chosen because this panel contains antibodies to the chemokines/cytokines previously identified to be differentially regulated by laboratory-attenuated and wt RABV (10). As shown in Fig. 3.5, 25 out of 30 chemokines/cytokines were significantly produced in the brains of mice infected with CVS-B2c than in mice infected with DRV-Mexico (Fig. 3.5). These include chemokines (CXCL10, CXCL9, CXCL2, CXCL1, CCL11, CCL5, CCL4, CCL3, and CCL2), interleukins (IL-1 α , IL-17, IL-13, IL-12, IL-7, IL-6, and IL-5) and growth factors (VEGF, CSF3, CSF2, CSF1, and LIF). Most of these cytokines were up-regulated by day 6 p.i. and continued to increase by day 9 p.i., while others (CXCL2, IFN- γ , CSF1, and LIF) were only up-regulated by day 9 p.i., indicating that they might be subsequently induced by other cytokines. The increase of CXCL10 was so much that it was out of the detection range in the brain extracts prepared from mice infected with CVS-B2c. Production of cytokines involved in Th1 signaling pathway such as IFN- γ and IL-12 were significantly elevated in mice infected with CVS-B2c, while secretion of IL-4 and IL-10 involved in Th2 signaling pathway remained unchanged in all groups.

Molecular networks of differentially expressed genes in the CNS exposed to RABV. Luminex data were further analyzed with IPA to map the networks of chemokines/cytokines expressed in the brains of mice infected with CVS-B2c or DRV-Mexico. Chemokines/cytokines were mapped into genetic networks with related molecules in different signaling pathways in IPA database and the pathways were ranked by scores. The higher a score, the lower the chance a network is achieved by random chance alone. Our analysis generated a network of CVS-B2c with a score of 59 and a network of DRV-Mexico with a score of 26. These pathways contain 26 and 12 focus molecules, respectively. In the molecular network generated from the group of mice infected with CVS-B2c, IFN- γ locates in the center and is directly linked

with CXCL10, CXCL9, CCL5, IL-17, IL-12, IL-6, and VEGF (Fig. 3.6A). In contrast, TNF- α locates in the center of network generated from mice infected with DRV-Mexico and connects with CCL11 and CXCL10 (Fig. 3.6B).

Neutralization of IFN- γ ameliorated disruption of BBB integrity and down-regulation of TJ proteins. IPA data described above indicate that IFN- γ plays a central role in the enhancement of BBB permeability in infection with laboratory-attenuated RABV. To investigate if disrupting IFN- γ function inhibits the enhancement of BBB permeability in mice infected with laboratory-attenuated RABV, anti-IFN- γ neutralizing antibodies were injected i.p. into mice at days 0, 2, and 4 after infection with B2c. NaF uptake was measured at day 6 p.i.. Isotype antibody was included as control. As shown in Fig. 3.7, treatments with anti-IFN- γ antibody significantly ameliorated enhancement of BBB permeability both in cerebrum and cerebellum while treatment with isotype controls had no impact on the enhancement of BBB permeability. To test if anti-IFN- γ antibody blocks down-regulation of TJ protein expression, bEnd.3 cells treated with a mixture of anti-IFN- γ antibody and brain extract prepared from mice infected with B2c (10LD50). It was found that expressions of claudin-5 and occludin in bEnd.3 cells treated with the mixture of anti-IFN- γ antibody and mouse brain extract were indistinguishable from sham-treated cells. Expressions of claudin-5 and occludin were significantly elevated in bEnd.3 cells inoculated with brain extract mixed with anti-IFN- γ antibody when compared with in cells treated with brain extract mixed with isotype control antibody (Fig. 3.7C and 3.7D). Taken together these results suggest that IFN- γ is a critical mediator of BBB permeability enhancement and TJ protein expression after infection with laboratory-attenuated RABV.

V. Discussion

The presence of BBB provides a physical and physiological barrier for cells and molecules to enter into the CNS (20, 22, 23) and thus enhancement of BBB permeability has often been associated with pathological changes in the CNS (19). However, transiently increased BBB permeability has been associated with clearance of RABV from the CNS and prevention from developing rabies (13). Laboratory-attenuated RABVs including those expressing multiple copies of the G (17) and immune stimulating molecules (18) can transiently enhance BBB permeability in mouse model as early as day 6 after infection. On the other hand, wt RABV does not induce enhancement of BBB permeability (6, 10, 13). Since TJ proteins are important in maintaining BBB integrity, TJ protein expression was investigated *in vitro* and *in vivo* after intracranial infection with laboratory-attenuated or wt RABV in the present study. The expression levels of TJ proteins were found to be reduced in the brains of mice infected with laboratory-attenuated, but not wt, RABV. Furthermore, *in vitro* studies with BMECs indicate that the reduction in TJ protein expression is not directly caused by RABV infection per se, but by chemokines/cytokines induced by infection with laboratory-attenuated RABV.

ECs are the major components of the BBB and TJ proteins present on and between the ECs form a barrier that maintains homeostasis of the CNS by restricting diffusion of blood-borne molecules (38). Alteration of TJ protein expression has been observed in viral infections (MAV-1) or autoimmune diseases (EAE) (26, 28). The mRNA and proteins for ZO-2, claudin-5, and occludin are reduced in ECs infected with MAV-1 (26). In EAE, claudin-5 and occludin are

both down-regulated and claudin-5 has been shown to be the key determinant for BBB breakdown (39). Reduction of TJ proteins at the impaired BBB and influx of encephalitogenic T cells generate plaques in the brain parenchyma, resulting in exacerbation of EAE (40). However, enhanced BBB permeability has been shown to be beneficial for RABV infection since permeable BBB allows immune effectors to enter the CNS, to clear RABV from the CNS, and to prevent experimental animals from developing rabies (10, 41). However, the mechanisms by which laboratory-attenuated RABV enhances BBB permeability were not known. Our present study shows that significantly decreased expression of TJ protein (claudin-5, occludin, and ZO-1) is observed in mice infected with laboratory-attenuated RABV, which corresponds to the enhancement of BBB in these animals. Little to no reduction of TJ protein expression was found in the brain of mice infected with wt RABV and no enhancement of BBB permeability was found in these animals until the end stage of disease. The reduction of TJ protein expression has recently been reported in rats infected with RABV (42). However, only the expression of occludin, but not ZO-1, was found to be reduced in infected animals. This discrepancy may have been due to the different animal models used. In Liao et al (42), the LEW/SsN^Narl rat used in that study is an inbred strain that may possess allelic loci impacting RABV severity in rat (43), while the ICR mouse used in the present study is an outbred strain that mimics genetic diversity of the human population.

Many host and viral factors contribute to the disruption of BBB integrity (19). In HIV, alteration of occludin and ZO-1 expression at the BBB has been demonstrated to be viral gp120- and CCL2-dependent (44-47). In EAE, IL-17 signaling is crucial for reduction in TJ proteins and trafficking of encephalitogenic T cells to the brain (48, 49). MAV-1 infects ECs and directly

damages TJ proteins, so alteration of TJ proteins is cytokine-independent (26). Our data show that RABV does not infect human or mouse ECs *in vitro* as detected by viral antigen expression or viral RNA replication. Likewise, RABV does not damage TJ proteins in these cells. To investigate what induced the reduction of TJ protein expression in RABV-infected mice, brain extracts were prepared from mice infected with laboratory-attenuated CVS-B2c or wt DRV-Mexico. Expression of claudin-5 and occludin decreased significantly in ECs when incubated with brain extracts derived from mice at day 6 and 9 after infection with laboratory-attenuated RABV, while the expression of TJ proteins showed some reduction only in ECs co-cultured with brain extracts prepared from mice at day 9 after infection with wt RABV. These results are consistent with enhancement of BBB permeability in mice, i.e. enhancement of BBB permeability was observed in mice infected with laboratory-attenuated, but not with wt, RABV in this study as well as in previous studies (6, 8). Therefore, the disruption of TJ proteins and enhancement of BBB permeability are not due to direct RABV infection, but due to the molecules in the brain extracts induced by laboratory-attenuated RABV.

To analyze the molecules in the brain extracts induced by RABV infection that are associated with the reduction of TJ protein expression, Milliplex MAP 30-plex premixed mouse cytokine/chemokine magnetic bead panel was used to measure the levels of chemokines/cytokines in the mouse brain. This panel was selected because previous studies have indicated that elevated innate immunity was found in the CNS of mice infected with laboratory-attenuated RABV (6, 10). Recombinant RABV expressing chemokine (CXCL10, CCL5, or CCL3) induced the enhancement of BBB permeability in mice (7) and reduced the expression of TJ proteins in BMECs as shown in this study. Furthermore, enhancement of BBB permeability is

chemokine/cytokine-dependent in many diseases (19). For example, in HIV infection, CCL2 was demonstrated to reduce the expression of ZO-1, ZO-2, occludin, and claudin-5 in ECs through Rho and Rho kinase signaling (50). In EAE, IL-17-induced reactive oxygen species activates myosin light chain kinase and reduces expression levels of ZO-1 and occludin in bEnd.3 cells (28). Indeed, our Luminex data showed that brain extracts from mice infected with laboratory-attenuated RABV contained significantly higher levels of chemokines/cytokines than those from mice infected with wt RABV. These include CXCL10, CXCL1, CCL11, CCL5, CCL4, CCL3, CCL2, IL-1 α , IL-17, IL-12, IL-6, IL-5, and IFN- γ . These results suggest that these elevated chemokines/cytokines could be responsible for the reduction of TJ protein expression and consequently the enhancement of BBB permeability in mice infected with laboratory-attenuated RABV.

To decipher the pathway(s) by which chemokines/cytokines reduce the expression of TJ proteins, analysis of molecular networks associated with differentially expressed genes is performed in the present study. In mice infected with laboratory-attenuated RABV, IFN- γ locates in the center of the molecule network. It has been reported that IFN- γ , but not TNF- α , was demonstrated to be associated with enhanced BBB permeability through ONOO⁻ dependent pathway in RABV infection *in vitro* (32). By neutralizing IFN with antibodies, the enhancement of BBB permeability can be ameliorated in mice and the down-regulation of TJ proteins can be blocked in ECs infected with laboratory-attenuated RABV. These studies further confirm that indeed IFN- γ plays a central role in enhancing BBB permeability in mice infected with laboratory-attenuated RABV. Pathway analysis also indicates that IFN directly connects with the most highly expressed chemokine, CXCL10. Although only low level of IFN- γ was detected at

day 6 p.i., it is highly expressed at the later stage of infection (day 9 p.i.). Thus, CXCL10 could be the initiation factor for reduction in TJ protein expression and enhancement of BBB permeability in mice infected with laboratory-attenuated RABV. Recombinant RABV expressing CXCL10 also significantly enhanced BBB permeability as shown in previous studies (7). Immunofluorescence data in our study showed substantial reduction in occludin and claudin-5 in BMECs incubated with supernatant containing CXCL10. CXCL10 can be secreted by brain resident cells such as neurons, microglial cells, and astrocytes (51, 52), it can also be produced by immune cells influx from the periphery (53). For WNV infection, it is neuronal CXCL10 that initiates influx of CD8⁺ T cells into the CNS. Neutralization of CXCL10 decreases the number of CD8⁺ T cells in the brain and elevates mortality (52). It is not clear, however, whether it is resident neural cells or cells infiltrated from the periphery that produce CXCL10 and initiate alteration of TJ proteins at the BBB after RABV infection.

In mice infected with wt RABV, TNF- α locates in the center of the molecule network. TNF- α has been shown to induce BBB disruption as a result of decreased TEER of microvascular ECs (54). Intraventricular injection of TNF- α in rat initiated an increased efflux of radio-labeled albumin into the CSF (55). However, Saija reported that intracarotid injection of TNF- α produced a significant decrease in BBB permeability to aminoisobutyric acid in rat (56). Others have shown that intracerebral injection of TNF- α does not alter BBB permeability in mice or rats (57, 58). The effects of TNF- α on BBB permeability in RABV infection are not clear (59, 60). CXCL10 is also up-regulated in mice infected with DRV-Mexico; however, the expression level of CXCL10 was significantly lower than that in mice infected with CVS-B2c. Although CXCL10 can be stimulated by TNF- α (61), the expression level of CXCL10 remains low in mice

infected with DRV-Mexico, this is possibly due to the lack of IFN- γ (61). In contrast, significantly high level of CXCL10 was generated with the cooperation of IFN- γ and TNF- α as shown in network constructed in CVS-B2c-infected group (Fig. 3.6A).

CXCL10, CXCL9 and CCL5 are three structurally and functionally related IFN- γ inducible proteins, they bind to receptor CXCR3 expressed on activated CD4⁺ Th1 cells and function in governing migration of lymphocytes into the CNS (62, 63). There is a crosstalk between IFN- γ , IL-12, and encephalitogenic CD4⁺ Th1 signaling pathways (48). Thus, Th1 signaling pathway may play an important role in the enhancement of BBB permeability in mice infected with laboratory-attenuated RABV. Furthermore, analysis of canonical pathways in our study suggests that differential regulation of IL-17A production and IL-17A may be a key event in BBB enhancement observed in mice infected with laboratory-attenuated RABV. Therefore, we hypothesize that infection with RABV, particularly laboratory-attenuated RABV, in the CNS stimulates the production of CXCL10 (other chemokines such as CCL5 and CCL3 may also be involved) in neural cells. These chemokines attract CXCR3+CD4⁺ T cells infiltrating into the CNS along the chemokine gradient and differentiating to IL-17-producing Th17 cells and IFN-producing Th1 cells. This process has been shown to be the exclusive way of leukocyte-skewing process in the CNS inflammation (29). IL-17 produced by Th17 cells in the CNS initiates the alteration of TJ proteins in RABV infection. IFN- γ secreted by Th1 cells promotes the loop of positive feedback and amplifies CXCL10 production, CXCR3+CD4 T cells influx and breakdown of the BBB (Fig. 3.8). The detection of significantly expressed IFN- γ at the later stage of infection further supports this hypothesis. Nevertheless, further studies are needed to demonstrate these pathways.

Figure 3.1

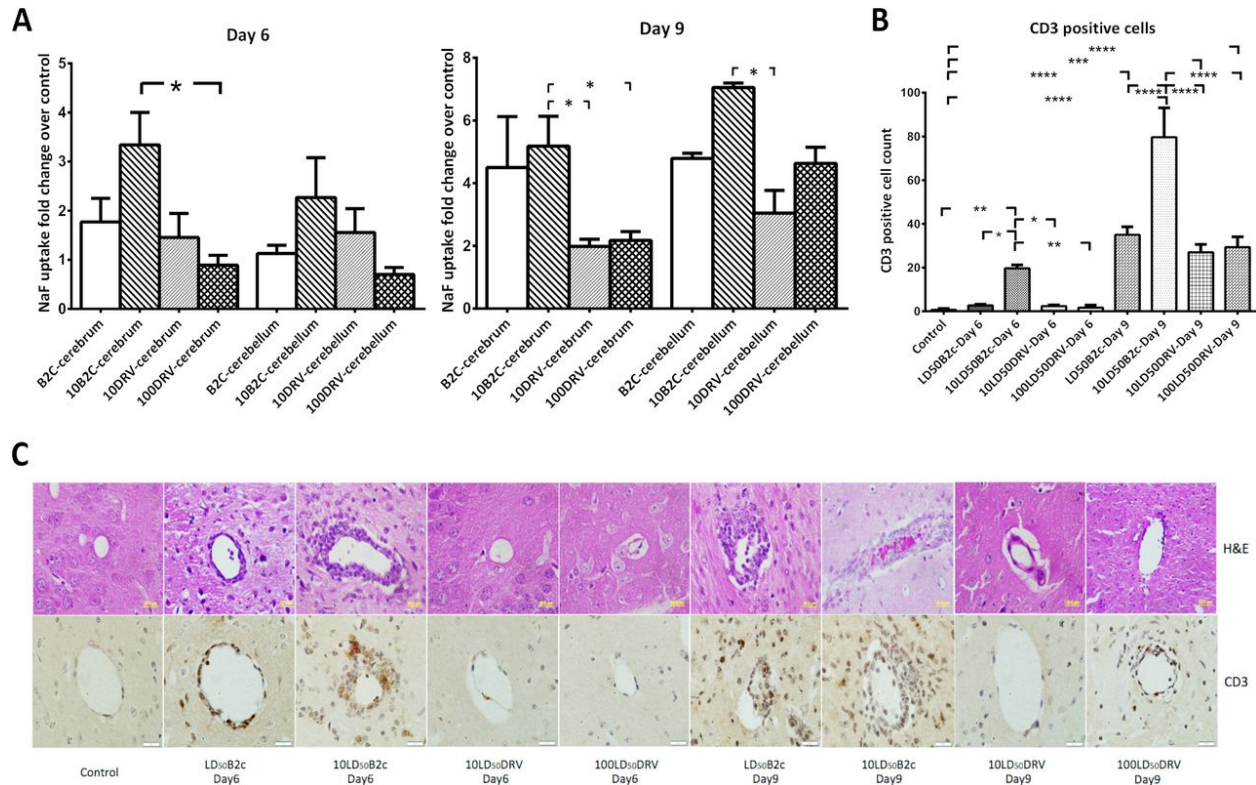


Fig. 3.1. NaF uptake and inflammatory cell infiltration in the CNS of mice infected with lab-attenuated CVS-B2c or wt DRV-Mexico. Female ICR mice were infected i.c. with 1 or 10 LD₅₀ of CVS-B2c, 10 or 100 LD₅₀ of DRV-Mexico. At day 6 or 9 p.i., BBB permeability was assessed by NaF uptake in the cerebrum and the cerebellum (A). Harvested brains were subjected to HE staining for histopathology as well as IHC for detection of CD3⁺ T cells (B). The CD3⁺ T cells (C) were quantified and analyzed statistically. Data are presented as mean ± SEM from three independent experiments. Statistics in panel A and C are repeated-measure

ANOVA with Tukey's post hoc test, and asterisk indicate the statistical significance. *, $P < 0.05$;

** , $P < 0.01$; *** , $P < 0.001$; **** , $P < 0.0001$.

Figure 3.2

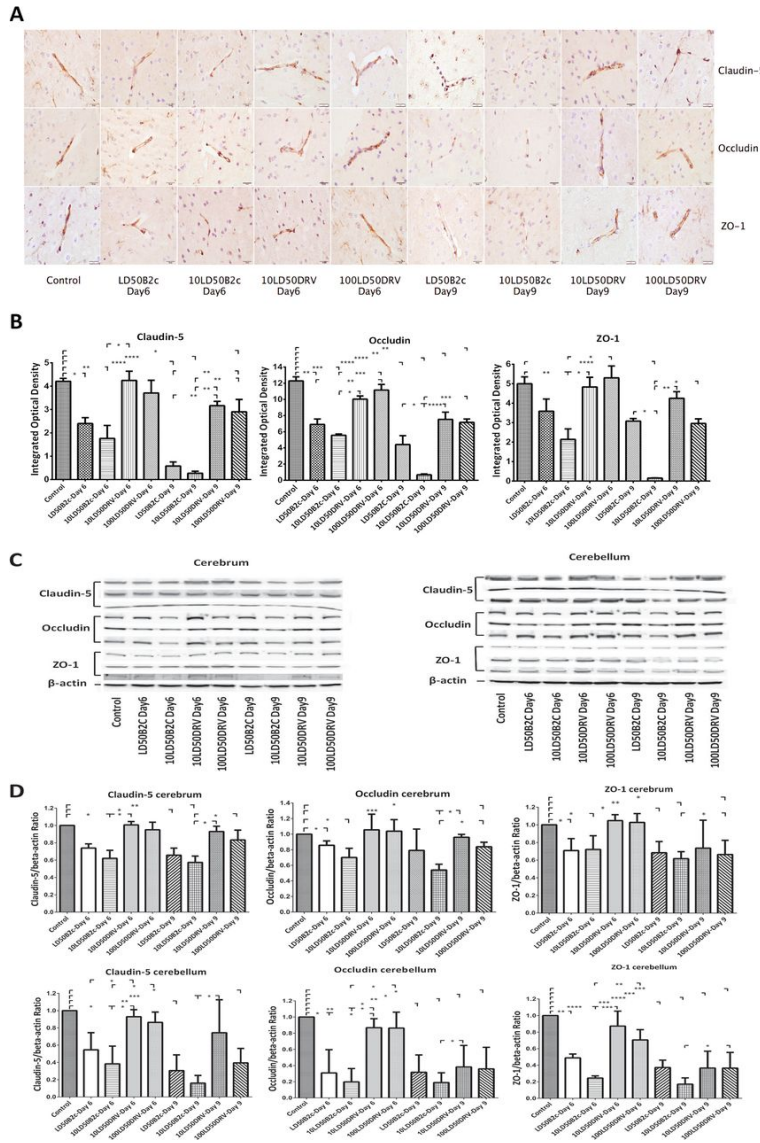


Fig. 3.2. Expression of TJ proteins (claudin-5, occludin, and ZO-1) in the brains of mice infected with CVS-B2c or DRV-Mexico. Mice were infected i.c. with 1 or 10 LD₅₀ of CVS-B2c, 10 or 100 LD₅₀ of DRV-Mexico. At day 6 or 9 p.i., animals were euthanized and brains were harvested, fixed, and sectioned for measuring the expression of TJ proteins using IHC with

antibodies to respective TJ proteins (A). The expression level of individual TJ protein was estimated by quantifying IODs and analyzed statistically (B). The expression of TJ proteins in RABV-infected mouse brains was confirmed by quantitative Western blotting (C). Quantitative Western blotting analyses of TJ protein expressions in brain extracts derived from mice infected with either virus (CVS-B2c or DRV-Mexico), sham-infected mice were the control (D). Data are presented as mean \pm SEM from three independent experiments. Statistics in panels B and D are repeated-measure ANOVA with Tukey's post hoc test, asterisk indicate the statistical significance. *, $P < 0.05$; **, $P < 0.01$; ***, $P < 0.001$; ****, $P < 0.0001$.

Figure 3.3

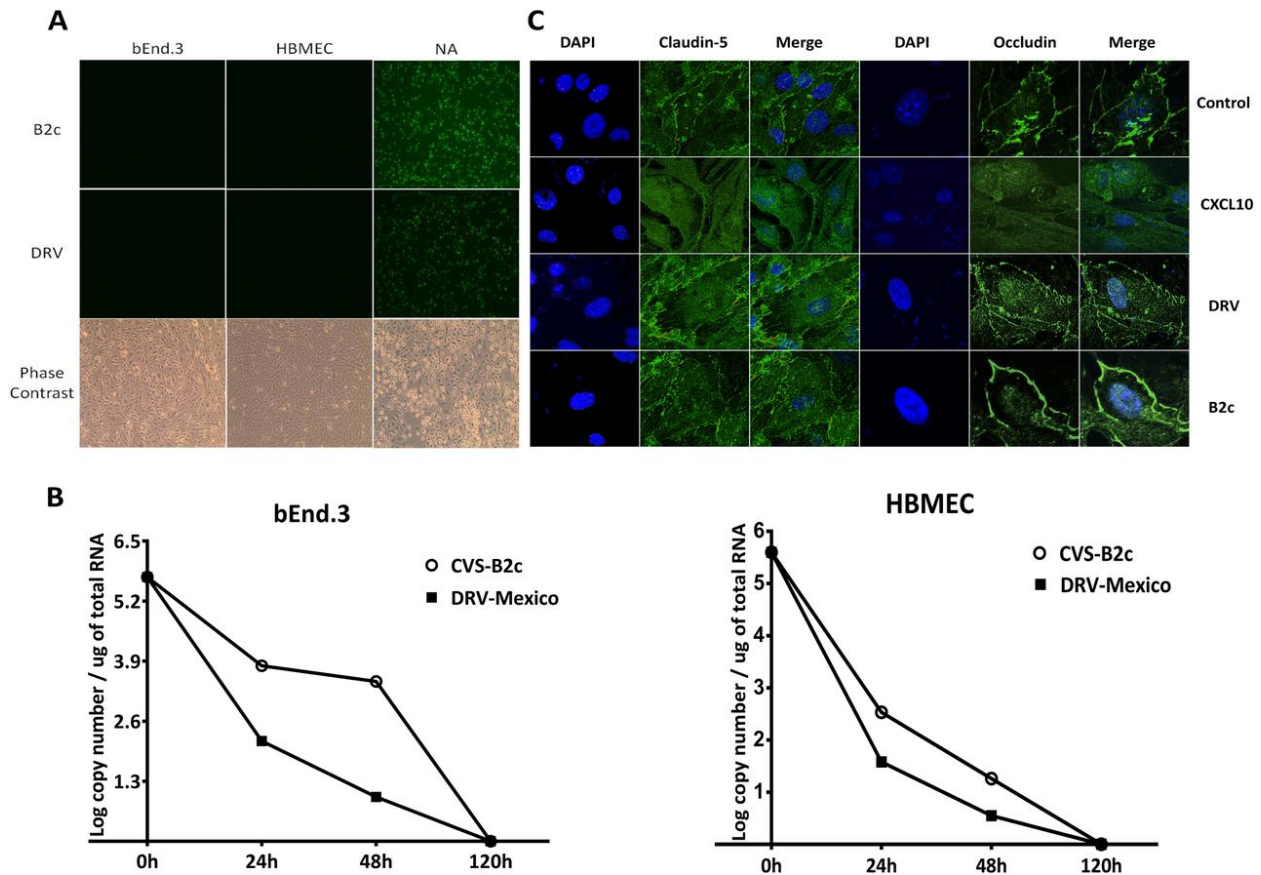


Fig. 3.3. Infection of human or mouse BMECs with RABVs and their effects on TJ protein expression. Human or mouse BMECs were co-cultured with CVS-B2c or DRV-Mexico at an MOI of 1, cells were fixed at 120 h after inoculation to assess active viral replication using FITC-conjugated anti-RABV N antibodies (A). mRNA cells infected with each virus were included as positive controls. Phase contrast microscopy was performed to ensure cell viability and structure (A). Culture supernatants were collected at 0, 24, 48, and 120 h, quantitative RT-

PCR was carried out to measure viral genome copy number post inoculation (B). The expression of TJ proteins was detected with antibodies to TJ proteins on BMEC cells co-cultured with either virus using confocal microscopy (C). BMECs co-cultured with the supernatant of mNA cells infected with rHEP-CXCL10 were included as a positive control.

Figure 3.4

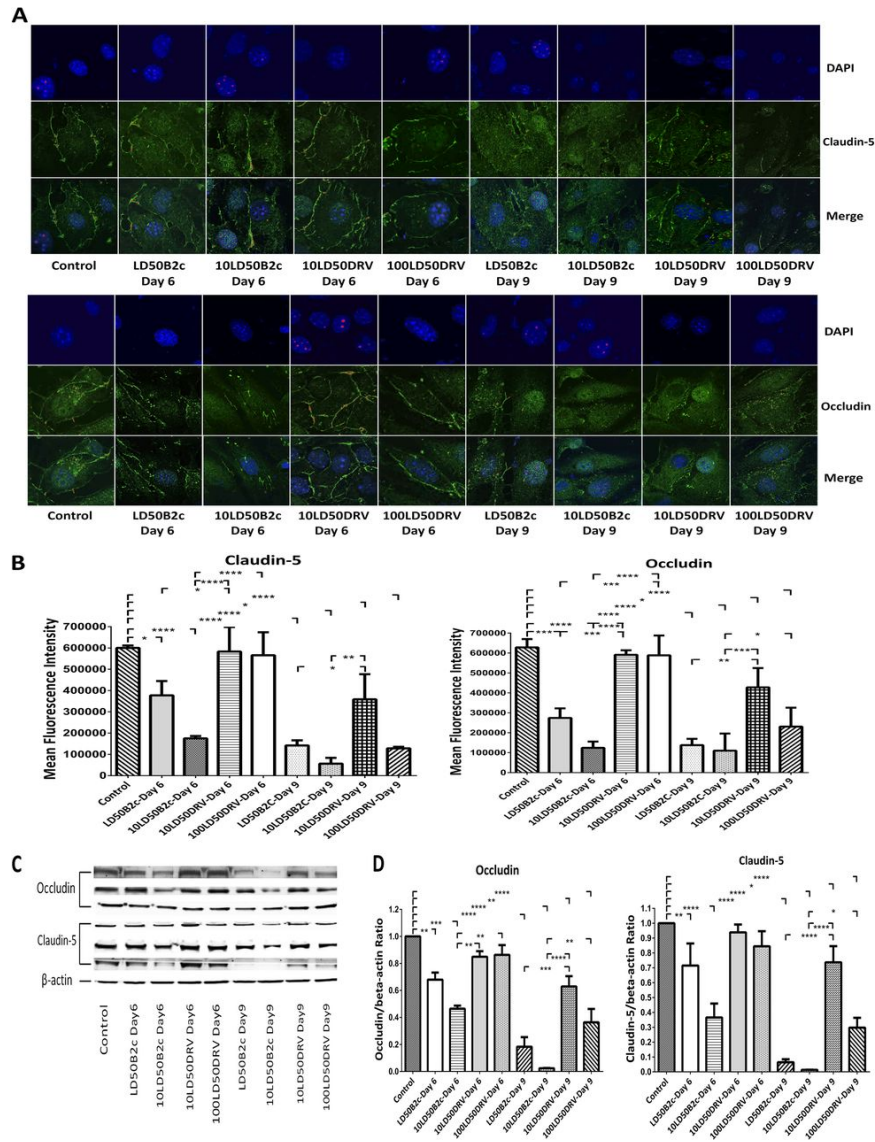


Fig. 3.4. The effects of brain extracts derived from mice infected with CVS-B2c or DRV-Mexico on the expression of TJ proteins in BMECs. Mouse BMECs were co-cultured with brain extracts derived from mice infected with different doses of CVS-B2c or DRV-Mexico.

After 24 h, BMECs were fixed and stained with DAPI and anti-claudin-5 antibody or DAPI and anti-occludin antibody (A). The staining was visualized by confocal microscopy. Panel B shows the MFI at ROI drawn around the cells under each condition (B). The expression of TJ proteins in BMECs after co-culturing with brain extracts was also detected using quantitative Western blotting (C). Quantitative Western blotting analyses of TJ protein expressions in BMECs treated with brain extracts derived from mice infected with either virus (CVS-B2c or DRV-Mexico), bEnd.3 cells treated with brain extracts derived from sham-infected mice were the control (D). Data are presented as mean \pm SEM from three independent experiments. Statistics in panel B and D are repeated-measure ANOVA with Tukey's post hoc test, asterisk indicate the statistical significance. *, P < 0.05; **, P < 0.01; ***, P < 0.001; ****, P < 0.0001.

Figure 3.5

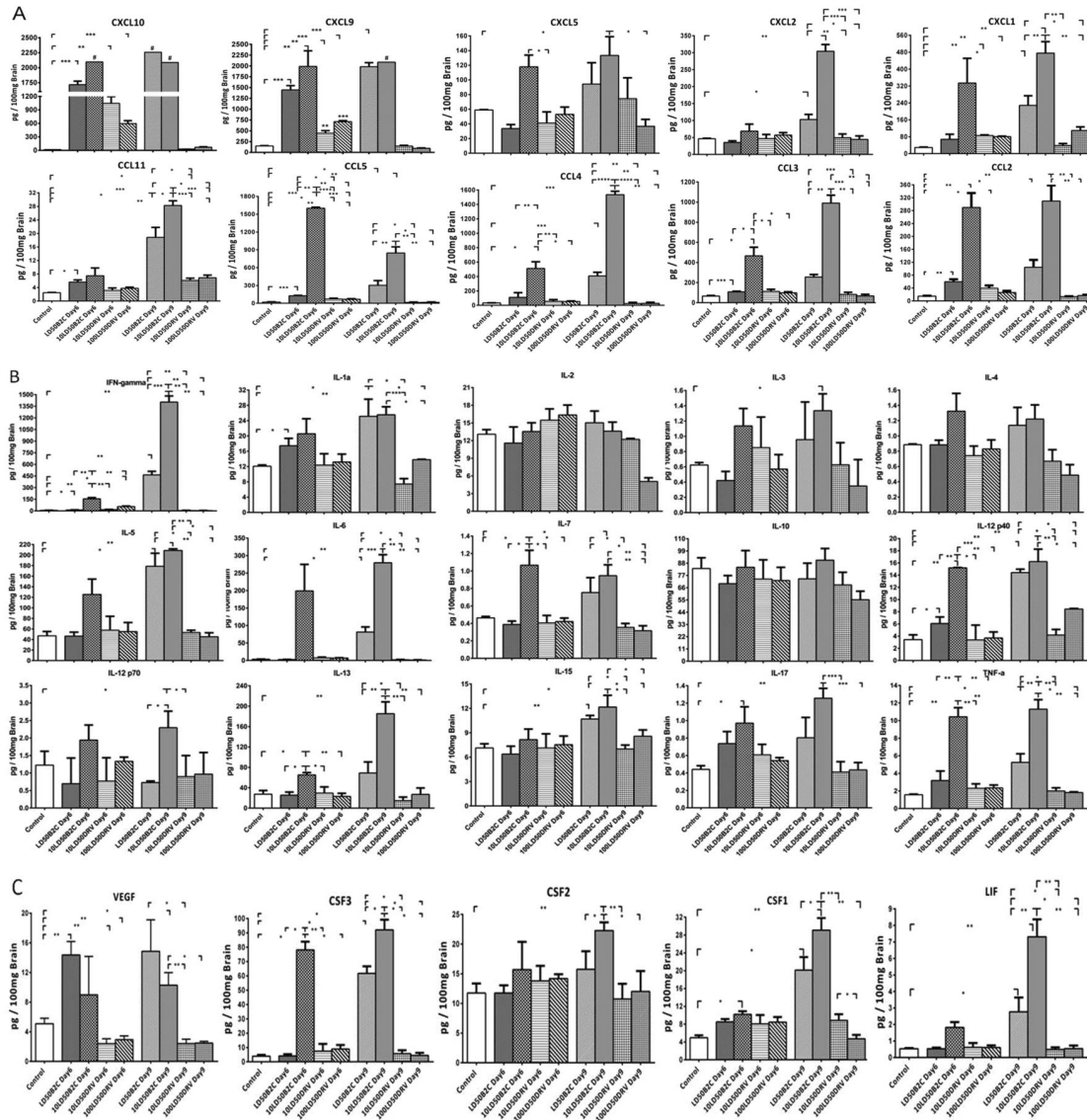


Fig. 3.5. Measurement of cytokines in the brain extracts derived from mice infected with CVS-B2c or DRV-Mexico by Luminex assay. ICR mice were infected i.c. with 1 or 10 LD₅₀ of CVS-B2c, 10 or 100 LD₅₀ of DRV-Mexico. At day 6 or 9 p.i., animals were euthanized and

brains were harvested and homogenized. After centrifugation, the supernatants were loaded to measure the concentrations of indicated cytokines using Luminex assay. Expression levels of chemokines were shown in panel A. Expression levels of interleukins, TNF- α , and IFN- γ were shown in panel B. Expression levels of growth factors were shown in panel C. Experiments were performed with three mouse replicates for each time point and condition. Hash tags indicate expression levels of cytokines beyond the upper detection range. Data are presented as mean \pm SEM from three independent experiments. Statistics in panels A, B, and C are repeated-measure ANOVA with Tukey's post hoc test, asterisk indicate the statistical significance. *, P < 0.05; **, P < 0.01; ***, P < 0.001; ****, P < 0.0001.

Figure 3.6

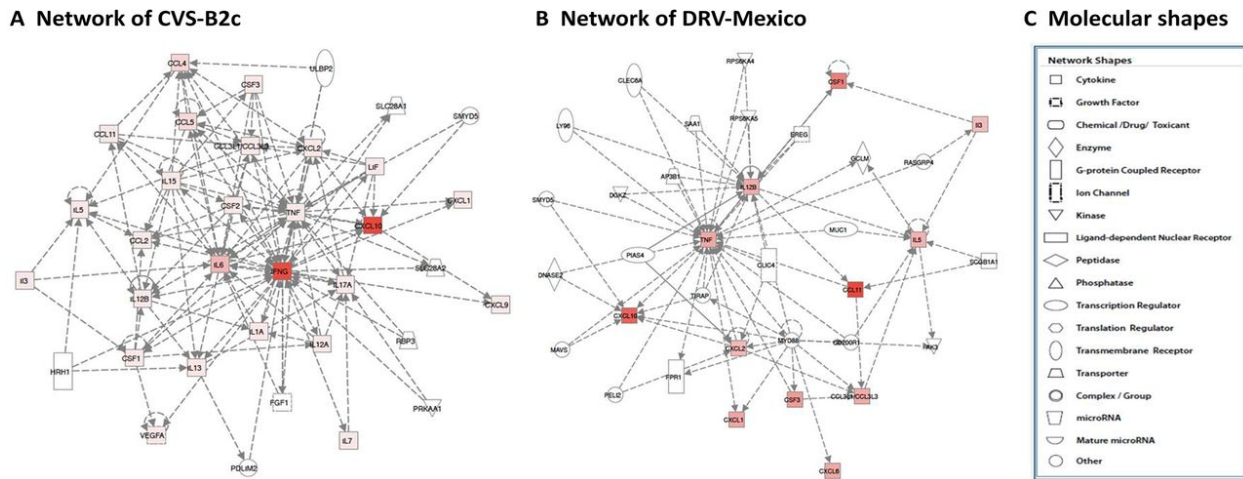


Fig. 3.6. Ingenuity Pathways Analysis of immune response, regulatory networks, and pathways mediated by infection with CVS-B2c or DRV-Mexico. The data generated by Luminex assay was analyzed with IPA software. One network of genes expressed in the brain of mice infected with CVS-B2c (A) and one network in the CNS of mice infected with DRV-Mexico (B) were established. Nodes represent genes, their shape represents the functional class of the gene product, and their edges indicate the biologic relationship between the nodes (C). The intensity of node colors indicates the degree of up- (red) or down-regulation (green) in mice inoculated with either RABV. White (noncolored) nodes are nonfocus genes that are biologically relevant to the pathways but not identified as differentially expressed in our Luminex analysis.

Figure 3.7

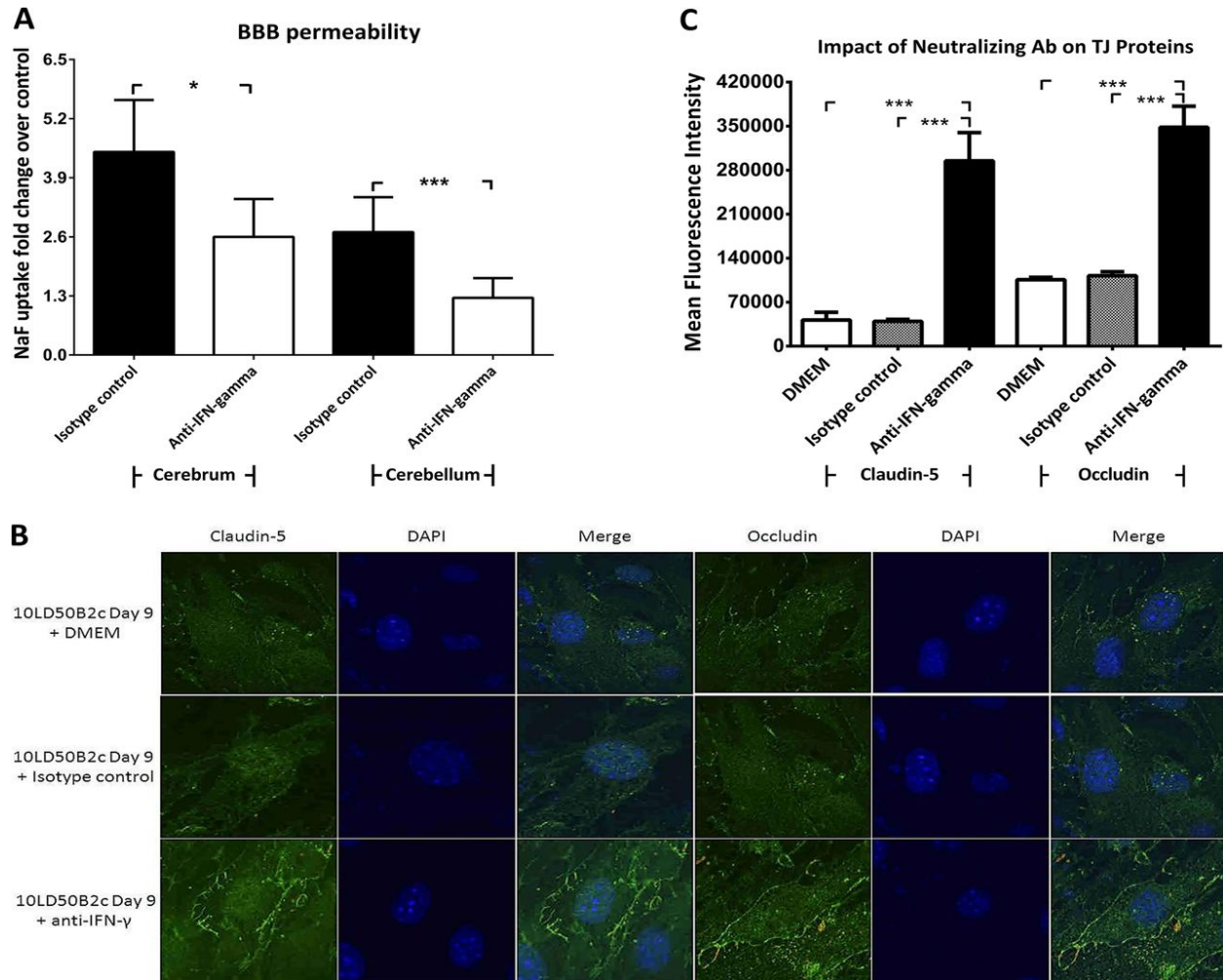


Fig. 3.7. (A and B) IFN- γ neutralization ameliorates the enhancement of BBB permeability in RABV-infected mice (A) and the downregulation of TJ protein expression in BMECs treated with brain extracts from RABV-infected mice (B). (A) Female ICR mice infected i.c. with 10 LD₅₀ of CVS-B2c were injected i.p. with 100 μ g of an anti-IFN- γ neutralizing antibody or an isotype control antibody in PBS at 0, 2, and 4 days p.i. At day 6 p.i., BBB permeability was

assessed by NaF uptake in the cerebrum and the cerebellum. Statistical analysis was performed with Student's *t* test. (B) Mouse BMECs were cocultured with brain extracts (treated either with DMEM, with 0.3 µg/ml of an anti-IFN-γ antibody, or with an isotype control antibody) from mice infected with 10 LD₅₀ of CVS-B2c. After 24 h, BMECs were fixed and were stained either with DAPI and an anti-claudin-5 antibody or with DAPI and an anti-occludin antibody. The staining was visualized by confocal microscopy. (C) The MFIs at the ROI drawn around the cells under the different conditions were compared and analyzed statistically using one-way ANOVA followed by Tukey's *post hoc* test. Asterisks indicate statistical significance (*, $P < 0.05$; **, $P < 0.01$; ***, $P < 0.001$; ****, $P < 0.0001$).

Figure 3.8

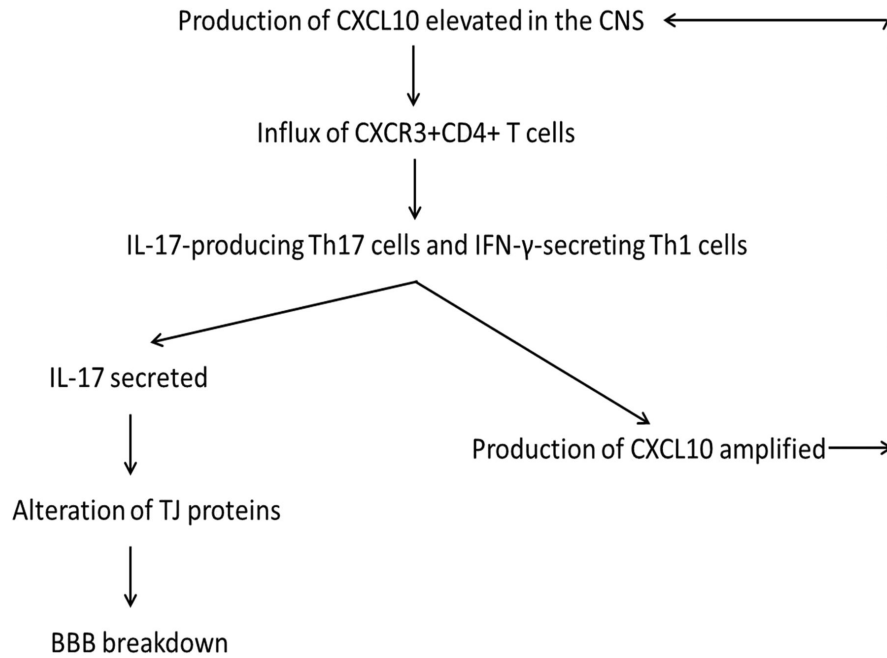


Fig. 3.8. Schematic model for the mechanism(s) by which infection with laboratory-attenuated RABV induces the reduction of TJ protein expression and the enhancement of BBB permeability.

VI. References

1. **Knobel DL, Cleaveland S, Coleman PG, Fevre EM, Meltzer MI, Miranda ME, Shaw A, Zinsstag J, Meslin FX.** 2005. Re-evaluating the burden of rabies in Africa and Asia. *Bulletin of the World Health Organization* **83**:360-368.
2. 2005. WHO Expert Consultation on rabies. World Health Organization technical report series **931**:1-88, back cover.

3. **Rupprecht CE.** 1996. Rhabdoviruses: Rabies Virus. *In* Baron S (ed.), Medical Microbiology, 4th ed, Galveston (TX).
4. **Schnell MJ, McGettigan JP, Wirblich C, Papaneri A.** 2010. The cell biology of rabies virus: using stealth to reach the brain. *Nature reviews. Microbiology* **8**:51-61.
5. **Suja MS, Mahadevan A, Madhusudana SN, Shankar SK.** 2011. Role of apoptosis in rabies viral encephalitis: a comparative study in mice, canine, and human brain with a review of literature. *Pathology research international* **2011**:374286.
6. **Kuang Y, Lackay SN, Zhao L, Fu ZF.** 2009. Role of chemokines in the enhancement of BBB permeability and inflammatory infiltration after rabies virus infection. *Virus research* **144**:18-26.
7. **Zhao L, Toriumi H, Kuang Y, Chen H, Fu ZF.** 2009. The roles of chemokines in rabies virus infection: overexpression may not always be beneficial. *Journal of virology* **83**:11808-11818.
8. **Roy A, Phares TW, Koprowski H, Hooper DC.** 2007. Failure to open the blood-brain barrier and deliver immune effectors to central nervous system tissues leads to the lethal outcome of silver-haired bat rabies virus infection. *Journal of virology* **81**:1110-1118.
9. **Jackson AC, Randle E, Lawrance G, Rossiter JP.** 2008. Neuronal apoptosis does not play an important role in human rabies encephalitis. *J Neurovirol* **14**:368-375.
10. **Wang ZW, Sarmiento L, Wang Y, Li XQ, Dhingra V, Tseggai T, Jiang B, Fu ZF.** 2005. Attenuated rabies virus activates, while pathogenic rabies virus evades, the host innate immune responses in the central nervous system. *Journal of virology* **79**:12554-12565.

11. **Sarmiento L, Tseggai T, Dhingra V, Fu ZF.** 2006. Rabies virus-induced apoptosis involves caspase-dependent and caspase-independent pathways. *Virus research* **121**:144-151.
12. **Yan X, Prośniak M, Curtis MT, Weiss ML, Faber M, Dietzschold B, Fu ZF.** 2001. Silver-haired bat rabies virus variant does not induce apoptosis in the brain of experimentally infected mice. *J Neurovirol* **7**:518-527.
13. **Hooper DC, Scott GS, Zborek A, Mikheeva T, Kean RB, Koprowski H, Spitsin SV.** 2000. Uric acid, a peroxynitrite scavenger, inhibits CNS inflammation, blood-CNS barrier permeability changes, and tissue damage in a mouse model of multiple sclerosis. *FASEB journal : official publication of the Federation of American Societies for Experimental Biology* **14**:691-698.
14. **Hooper DC, Morimoto K, Bette M, Weihe E, Koprowski H, Dietzschold B.** 1998. Collaboration of antibody and inflammation in clearance of rabies virus from the central nervous system. *Journal of virology* **72**:3711-3719.
15. **Bennett J, Basivireddy J, Kollar A, Biron KE, Reickmann P, Jefferies WA, McQuaid S.** 2010. Blood-brain barrier disruption and enhanced vascular permeability in the multiple sclerosis model EAE. *Journal of neuroimmunology* **229**:180-191.
16. **Kean RB, Spitsin SV, Mikheeva T, Scott GS, Hooper DC.** 2000. The peroxynitrite scavenger uric acid prevents inflammatory cell invasion into the central nervous system in experimental allergic encephalomyelitis through maintenance of blood-central nervous system barrier integrity. *Journal of immunology* **165**:6511-6518.

17. **Faber M, Li J, Kean RB, Hooper DC, Alugupalli KR, Dietzschold B.** 2009. Effective preexposure and postexposure prophylaxis of rabies with a highly attenuated recombinant rabies virus. *Proceedings of the National Academy of Sciences of the United States of America* **106**:11300-11305.
18. **Wang H, Zhang G, Wen Y, Yang S, Xia X, Fu ZF.** 2011. Intracerebral administration of recombinant rabies virus expressing GM-CSF prevents the development of rabies after infection with street virus. *PloS one* **6**:e25414.
19. **Spindler KR, Hsu TH.** 2012. Viral disruption of the blood-brain barrier. *Trends in microbiology* **20**:282-290.
20. **Abbott NJ, Patabendige AA, Dolman DE, Yusof SR, Begley DJ.** 2010. Structure and function of the blood-brain barrier. *Neurobiol Dis* **37**:13-25.
21. **Lehner C, Gehwolf R, Tempfer H, Krizbai I, Hennig B, Bauer HC, Bauer H.** 2011. Oxidative stress and blood-brain barrier dysfunction under particular consideration of matrix metalloproteinases. *Antioxidants & redox signaling* **15**:1305-1323.
22. **Rubin LL, Staddon JM.** 1999. The cell biology of the blood-brain barrier. *Annual review of neuroscience* **22**:11-28.
23. **Pardridge WM.** 1999. Blood-brain barrier biology and methodology. *J Neurovirol* **5**:556-569.
24. **Toborek M, Lee YW, Flora G, Pu H, Andras IE, Wylegala E, Hennig B, Nath A.** 2005. Mechanisms of the blood-brain barrier disruption in HIV-1 infection. *Cellular and molecular neurobiology* **25**:181-199.

25. **Mathur A, Khanna N, Chaturvedi UC.** 1992. Breakdown of blood-brain barrier by virus-induced cytokine during Japanese encephalitis virus infection. *International journal of experimental pathology* **73**:603-611.
26. **Gralinski LE, Ashley SL, Dixon SD, Spindler KR.** 2009. Mouse adenovirus type 1-induced breakdown of the blood-brain barrier. *Journal of virology* **83**:9398-9410.
27. **Murphy AC, Lalor SJ, Lynch MA, Mills KH.** 2010. Infiltration of Th1 and Th17 cells and activation of microglia in the CNS during the course of experimental autoimmune encephalomyelitis. *Brain, behavior, and immunity* **24**:641-651.
28. **Huppert J, Closhen D, Croxford A, White R, Kulig P, Pietrowski E, Bechmann I, Becher B, Luhmann HJ, Waisman A, Kuhlmann CR.** 2010. Cellular mechanisms of IL-17-induced blood-brain barrier disruption. *FASEB journal : official publication of the Federation of American Societies for Experimental Biology* **24**:1023-1034.
29. **Shechter R, London A, Schwartz M.** 2013. Orchestrated leukocyte recruitment to immune-privileged sites: absolute barriers versus educational gates. *Nature reviews. Immunology* **13**:206-218.
30. **Zhang G, Fu ZF.** 2012. Complete genome sequence of a street rabies virus from Mexico. *Journal of virology* **86**:10892-10893.
31. **Morimoto K, Hooper DC, Carbaugh H, Fu ZF, Koprowski H, Dietzschold B.** 1998. Rabies virus quasispecies: implications for pathogenesis. *Proceedings of the National Academy of Sciences of the United States of America* **95**:3152-3156.
32. **Phares TW, Fabis MJ, Brimer CM, Kean RB, Hooper DC.** 2007. A peroxynitrite-dependent pathway is responsible for blood-brain barrier permeability changes during a

- central nervous system inflammatory response: TNF-alpha is neither necessary nor sufficient. *Journal of immunology* **178**:7334-7343.
33. **Trout JJ, Koenig H, Goldstone AD, Lu CY.** 1986. Blood-brain barrier breakdown by cold injury. Polyamine signals mediate acute stimulation of endocytosis, vesicular transport, and microvillus formation in rat cerebral capillaries. *Laboratory investigation; a journal of technical methods and pathology* **55**:622-631.
 34. **Li XQ, Sarmiento L, Fu ZF.** 2005. Degeneration of neuronal processes after infection with pathogenic, but not attenuated, rabies viruses. *Journal of virology* **79**:10063-10068.
 35. **Zhang G, Wang H, Mahmood F, Fu ZF.** 2013. Rabies virus glycoprotein is an important determinant for the induction of innate immune responses and the pathogenic mechanisms. *Veterinary microbiology* **162**:601-613.
 36. **Wen Y, Wang H, Wu H, Yang F, Tripp RA, Hogan RJ, Fu ZF.** 2011. Rabies virus expressing dendritic cell-activating molecules enhances the innate and adaptive immune response to vaccination. *Journal of virology* **85**:1634-1644.
 37. **Famakin B, Mou Y, Spatz M, Lawal M, Hallenbeck J.** 2012. Downstream Toll-like receptor signaling mediates adaptor-specific cytokine expression following focal cerebral ischemia. *J Neuroinflammation* **9**:174.
 38. **Pfeiffer F, Schafer J, Lyck R, Makrides V, Brunner S, Schaeren-Wiemers N, Deutsch U, Engelhardt B.** 2011. Claudin-1 induced sealing of blood-brain barrier tight junctions ameliorates chronic experimental autoimmune encephalomyelitis. *Acta Neuropathol* **122**:601-614.

39. **Argaw AT, Gurfein BT, Zhang Y, Zameer A, John GR.** 2009. VEGF-mediated disruption of endothelial CLN-5 promotes blood-brain barrier breakdown. Proceedings of the National Academy of Sciences of the United States of America **106**:1977-1982.
40. **Sporici R, Issekutz TB.** 2010. CXCR3 blockade inhibits T-cell migration into the CNS during EAE and prevents development of adoptively transferred, but not actively induced, disease. Eur J Immunol **40**:2751-2761.
41. **Zhao L, Toriumi H, Kuang Y, Chen HC, Fu ZF.** 2009. The Roles of Chemokines in Rabies Virus Infection: Overexpression May Not Always Be Beneficial. J Virol **83**:11808-11818.
42. **Liao PH, Yang HH, Chou PT, Wang MH, Chu PC, Liu HL, Chen LK.** 2012. Sufficient virus-neutralizing antibody in the central nerve system improves the survival of rabid rats. Journal of biomedical science **19**:61.
43. **Olofsson P, Johansson A, Wedekind D, Kloting I, Klinga-Levan K, Lu S, Holmdahl R.** 2004. Inconsistent susceptibility to autoimmunity in inbred LEW rats is due to genetic crossbreeding involving segregation of the arthritis-regulating gene *Ncf1*. Genomics **83**:765-771.
44. **Dallasta LM, Pisarov LA, Esplen JE, Werley JV, Moses AV, Nelson JA, Achim CL.** 1999. Blood-brain barrier tight junction disruption in human immunodeficiency virus-1 encephalitis. The American journal of pathology **155**:1915-1927.
45. **Toneatto S, Finco O, van der Putten H, Abrignani S, Annunziata P.** 1999. Evidence of blood-brain barrier alteration and activation in HIV-1 gp120 transgenic mice. Aids **13**:2343-2348.

46. **Eugenin EA, Osiecki K, Lopez L, Goldstein H, Calderon TM, Berman JW.** 2006. CCL2/monocyte chemoattractant protein-1 mediates enhanced transmigration of human immunodeficiency virus (HIV)-infected leukocytes across the blood-brain barrier: a potential mechanism of HIV-CNS invasion and NeuroAIDS. *The Journal of neuroscience : the official journal of the Society for Neuroscience* **26**:1098-1106.
47. **Boven LA, Middel J, Verhoef J, De Groot CJ, Nottet HS.** 2000. Monocyte infiltration is highly associated with loss of the tight junction protein zonula occludens in HIV-1-associated dementia. *Neuropathol Appl Neurobiol* **26**:356-360.
48. **Lovett-Racke AE, Yang Y, Racke MK.** 2011. Th1 versus Th17: are T cell cytokines relevant in multiple sclerosis? *Biochimica et biophysica acta* **1812**:246-251.
49. **Stromnes IM, Cerretti LM, Liggitt D, Harris RA, Goverman JM.** 2008. Differential regulation of central nervous system autoimmunity by T(H)1 and T(H)17 cells. *Nature medicine* **14**:337-342.
50. **Stamatovic SM, Keep RF, Kunkel SL, Andjelkovic AV.** 2003. Potential role of MCP-1 in endothelial cell tight junction 'opening': signaling via Rho and Rho kinase. *J Cell Sci* **116**:4615-4628.
51. **Tanuma N, Sakuma H, Sasaki A, Matsumoto Y.** 2006. Chemokine expression by astrocytes plays a role in microglia/macrophage activation and subsequent neurodegeneration in secondary progressive multiple sclerosis. *Acta Neuropathol* **112**:195-204.

52. **Klein RS, Lin E, Zhang B, Luster AD, Tollett J, Samuel MA, Engle M, Diamond MS.** 2005. Neuronal CXCL10 directs CD8+ T-cell recruitment and control of West Nile virus encephalitis. *Journal of virology* **79**:11457-11466.
53. **Devaraj S, Jialal I.** 2009. Increased secretion of IP-10 from monocytes under hyperglycemia is via the TLR2 and TLR4 pathway. *Cytokine* **47**:6-10.
54. **de Vries HE, Blom-Rosemalen MC, van Oosten M, de Boer AG, van Berkel TJ, Breimer DD, Kuiper J.** 1996. The influence of cytokines on the integrity of the blood-brain barrier in vitro. *Journal of neuroimmunology* **64**:37-43.
55. **Dickstein JB, Moldofsky H, Hay JB.** 2000. Brain-blood permeability: TNF-alpha promotes escape of protein tracer from CSF to blood. *American journal of physiology. Regulatory, integrative and comparative physiology* **279**:R148-151.
56. **Saija A, Princi P, Lanza M, Scalese M, Aramnejad E, De Sarro A.** 1995. Systemic cytokine administration can affect blood-brain barrier permeability in the rat. *Life Sci* **56**:775-784.
57. **Petito CK, Adkins B, Tracey K, Roberts B, Torres-Munoz J, McCarthy M, Czeisler C.** 1999. Chronic systemic administration of tumor necrosis factor alpha and HIV gp120: effects on adult rodent brain and blood-brain barrier. *J Neurovirol* **5**:314-318.
58. **Schnell L, Fearn S, Schwab ME, Perry VH, Anthony DC.** 1999. Cytokine-induced acute inflammation in the brain and spinal cord. *Journal of neuropathology and experimental neurology* **58**:245-254.

59. **Mark KS, Miller DW.** 1999. Increased permeability of primary cultured brain microvessel endothelial cell monolayers following TNF-alpha exposure. *Life Sci* **64**:1941-1953.
60. **Liu H, Luiten PG, Eisel UL, Dejongste MJ, Schoemaker RG.** 2013. Depression after myocardial infarction: TNF-alpha-induced alterations of the blood-brain barrier and its putative therapeutic implications. *Neuroscience and biobehavioral reviews* **37**:561-572.
61. **Ohmori Y, Hamilton TA.** 1995. The interferon-stimulated response element and a kappa B site mediate synergistic induction of murine IP-10 gene transcription by IFN-gamma and TNF-alpha. *Journal of immunology* **154**:5235-5244.
62. **Muller M, Carter S, Hofer MJ, Campbell IL.** 2010. Review: The chemokine receptor CXCR3 and its ligands CXCL9, CXCL10 and CXCL11 in neuroimmunity--a tale of conflict and conundrum. *Neuropathol Appl Neurobiol* **36**:368-387.
63. **Liu L, Huang D, Matsui M, He TT, Hu T, Demartino J, Lu B, Gerard C, Ransohoff RM.** 2006. Severe disease, unaltered leukocyte migration, and reduced IFN-gamma production in CXCR3^{-/-} mice with experimental autoimmune encephalomyelitis. *Journal of immunology* **176**:4399-4409.

CHAPTER 4

EXPRESSION OF NEURONAL CXCL10 INDUCED BY RABIES VIRUS INFECTION INITIATES CHEMOKINES/CYTOKINES PRODUCTINO CASCADES AND BLOOD- BRAIN BARRIER DISRUPTION

Qingqing Chai, Ruiping She, Kasey Williams, Zhen F. Fu

To be submitted to Journal of Virology, 07/25/2014

I. Abstract

Previously, we showed that blood-brain barrier (BBB) disruption was modulated by expression of chemokines/cytokines and reduction of tight junction (TJ) proteins in the brains of mice infected with rabies virus (RABV), and CXCL10 has been found to be the most highly and earliest expressed in laboratory-attenuated RABV infection. In the present study, the temporal and spatial expression of CXCL10 was determined in RABV-infected mouse brain. Expression of CXCL10 was initially detected in neurons as early as day 3 post infection (p.i.) before it was detected in microglia (day 6 p.i.) and astrocytes (day 9 p.i.) in RABV-infected mice. Neutralization of CXCL10 reduced IFN- γ production, Th17 cell infiltration, loss of TJ protein expression, and the enhancement of BBB permeability in mice infected with laboratory-attenuated RABV. Thus we conclude neuronal CXCL10 induced by RABV initiates cascades leading to expression of other inflammatory chemokines/cytokines and enhancement of the BBB permeability.

II. Introduction

Rabies virus (RABV) continues to present public health threat, causing more than 55,000 human fatalities annually around the world (1, 2). In experimental animals, infection of wild type (wt) RABV results in higher morbidity and mortality than that of laboratory-attenuated RABV (3). This is because laboratory-attenuated RABV induces high levels of innate and

adaptive immunities and enhances BBB permeability that allows immune effectors to enter the central nervous system (CNS) and clears established infections (4, 5). Enhancement of BBB permeability is largely due to the expression of chemokines/cytokines induced by infection with laboratory-attenuated RABV (22). Pathway analysis indicates that IFN- γ located in the center of the molecule network relates to the up-regulation of chemokines/cytokines (6). Indeed, neutralizing IFN- γ with antibodies ameliorated enhancement of BBB permeability in infected mice. Up-regulation of IFN- γ occurred at the later stage of RABV infection (day 9 p.i.). However, IFN- γ inducible chemokine, CXCL10, was up-regulated the earliest and the most highly after infection with laboratory-attenuated RABV, leading to the hypothesis that CXCL10 might be the initiation factor for a cascade reaction resulting in the enhancement of BBB permeability (6).

CXCL10 is considered as one of the most potent chemoattractants for activated T cells and NK cells (7). CXCL10 receptor, CXCR3, is highly expressed on activated T cells, memory T cells and NK cells (8). It can be expressed by neurons, macrophages, CD14⁺ monocytes, astrocytes, T cells and endothelial cells (ECs) (9-12). In vitro studies have shown that macrophages stimulated with UV-inactivated RABV activate the extracellular signal-regulated kinase 1/2, subsequently inducing the expression of CXCL10 in macrophages (13). Astrocytes and microglia are also sources of CXCL10 after infection with many neurotropic viruses including mouse hepatitis virus (MHV), human immunodeficiency virus, Theiler's virus, and herpes simplex virus (14-16). Neutralization of astrocytes- and endothelial-derived CXCL10 successfully prevented BBB disruption and protective T cells from entering into the CNS in MHV infection (17). In EAE model, depletion of CXCL10 reduced BBB disruption and

infiltration of immune cells in the CNS, resulting in amelioration of clinical symptoms (18, 19). However, a study of EAE using CXCL10^{-/-} animals showed less improvement, which might be due to compensation of CXCL 9/11 expressions. CXCL 9/11 share the same cell surface receptor with CXCL10 and are induced by IFN- γ (20, 21). In the present study, the temporal and spatial expression as well as the function importance of CXCL10 on the enhancement of BBB permeability were investigated in mice after RABV infection (6).

III. Materials and Methods

Cells, viruses, antibodies and mice. Mouse brain microvascular EC (bEnd.3) was obtained from American Type Culture Collection (ATCC, Manassas, VA) and maintained in Dulbecco's Modified Eagle's Medium (DMEM) supplemented with fetal bovine serum (FBS) (ATCC). Mouse neuroblastoma (mNA) cells were maintained in RPMI 1640 medium (Mediatech, Herndon, VA) supplemented with 10% FBS. DRV-Mexico is a wt virus originated from a Mexican dog and propagated in suckling mouse brain (30). CVS-B2c is a laboratory-attenuated RABV by passaging the challenge virus standard (CVS-24) in baby hamster kidney (BHK21) cells. Fluorescein isothiocyanate (FITC)-conjugated anti-RABV-nucleoprotein antibody was obtained from FujiRebio (Malvern, PA). Rabbit polyclonal anti-occludin and anti-actin antibodies were obtained from Santa Cruz Biotechnology (Santa Cruz, CA). Anti-CXCL10 Antibody and mouse IgG1 isotype control antibody were purchased from R&D. Alexa-Fluor 488-conjugated goat anti-rabbit antibody was purchased from Invitrogen (Grand Island, NY). Female ICR mice (4-6 weeks old) were purchased from Harlan and housed in the animal facility

in the College of Veterinary Medicine, University of Georgia. All animal experiments were carried out under the Institutional Animal Care and Use Committee-approved protocols (animal welfare assurance No. A3058-01).

Measurement of BBB permeability. BBB permeability was determined by measuring Sodium Fluorescein (NaF) uptake as previously described (6). Briefly, NaF was used as the tracer; 100 μ l of 100 mg/mL of NaF was injected to each mouse through the tail vein. Peripheral blood was collected after circulation for 10 min and phosphate-buffered saline (PBS)-perfused brains were then harvested. Serum recovered was mixed with equal volume of 10% trichloroacetic acid (TCA) and then centrifuged for 10 min. The supernatant was collected after centrifugation and made up to 150 μ l by mixing with 5M NaOH and 7.5% TCA. Homogenized brain samples in cold 7.5% TCA were centrifuged for 10 min at 10,000 \times g to remove debris. The supernatant was made up to 150 μ l by adding 5M NaOH. The fluorescence of serum and brain homogenate samples was measured using a spectrophotometer (BioTek Instruments, VT) with excitation at 485 nm and emission at 530 nm. NaF taken up into brain tissues is expressed as the micrograms of fluorescence per mg of cerebrum or cerebellum divided by the micrograms of fluorescence per μ l of serum to normalize the uptake amounts of tracer from peripheral blood at the time of brain tissue collection (6). Data are expressed as a fold change in the amount of tracer in tissues by comparison with the values obtained for tissues from negative control.

Histopathology, immunohistochemistry (IHC), and quantitative Western blotting (WB) analysis. For histopathology and IHC, infected mice were anesthetized with ketamine-xylazine (0.1 ml/10 g body weight) and perfused with PBS followed by 10% neutral buffered

formalin as described previously (6). Three independent samples of mice brains were harvested from each group. Brain tissues were removed and paraffin-embedded for coronal sections (4 um). For IHC, the sections were deparaffinized and rehydrated in xylene and ethanol. Endogenous peroxidase was quenched by incubation in 5% hydrogen peroxide and antigen retrieval was performed in citrate buffer (Fisher Scientific, NH). Sections were then blocked with goat serum and incubated with primary antibodies overnight at 4°C and then biotinylated secondary antibodies. The avidin-biotin-peroxidase complex (VectaStain Standard ABC kit, Vector Laboratories, Burlingame, CA) was used to localize the biotinylated antibody. Diaminobenzidine (DAB, Vector Laboratories) was utilized for color development. Negative control was performed by substituting primary antibodies with PBS. For antigen quantification, sections were photographed and analyzed using Olympus BX41 Microscope (Tokyo, Japan). Integrated Optical Density (IOD) of DAB signals was determined by Image-pro Plus 4.5 software (Media Cybernetics, Bethesda, MD).

For WB, three independent samples of mouse brains from each group were collected, homogenized and prepared as 10% (w/v) suspension in DMEM. After centrifugation, the supernatants were collected and stored in -80°C. The brain extracts or cell lysates were subjected to 8%-16% sodium dodecyl sulfate polyacrylamide gel electrophoresis (SDS-PAGE) (Thermo Scientific, Rockford, IL). Separated proteins were electroblotted onto nitrocellulose membranes and incubated with primary antibodies overnight. After extensive washing with PBS, the blots were incubated with secondary antibodies. Proteins were detected by SuperSignal West Pico chemiluminescence (Thermo Scientific). Band signals corresponding to immunoreactive proteins

were captured and chemiluminescence intensities were analyzed using ChemiDoc 4000 MP documentation System (Biorad, CA).

Immunofluorescence and confocal microscopy. 10% (wt/vol) suspension of brain extract was prepared by homogenizing brain tissues in DMEM containing Complete Proteinase Inhibitor Cocktail (Roche, Germany). Brain homogenates were centrifuged to remove debris, and supernatants were harvested and seeded onto monolayers of bEnd.3 cells for 24 h. Cells were fixed and permeabilized with 0.2% Triton X-100. The expression of TJ protein was detected using primary anti-occludin or anti-claudin-5 antibodies. After washing, cells were incubated with Alexa-Fluor 488-conjugated goat anti-rabbit secondary antibody for 1 h at RT. Samples were mounted using Prolong Gold antifade reagent with DAPI (4', 6'-di-amidino-2-phenylindole) (Invitrogen, NY) and visualized with Nikon A1 Confocal Laser Microscope System equipped with NIS-Elements 4.13 imaging software (Melville, NY). The images recorded were quantified using NIH's Fiji (downloaded from pacific.mpi-cbg.de/wiki/index.php/fiji), a distribution package of ImageJ, The mean fluorescence intensity (MFI) was calculated using region of interest (ROI), which was drawn around an entire cell so that it always included the membrane. Three independent experiments were carried out for each condition. Background staining was accounted for by using three negatively stained regions per cell, which were subtracted from the total mean fluorescence.

Determination of cytokine expression in brain extracts. Extracts from homogenized brains were analyzed simultaneously for concentrations of IFN using ELISA kit (Biolegend, CA) according to the manufacturer's instructions. Precoated plate was filled with equal volume of

brain extracts in 96-well plates. Plates were protected from light and incubated on an orbital shaker overnight at 4°C, and magnetic beads were washed with 200 uL of wash buffer for three times. Then detection antibodies were added to each well and incubated at RT for 1 h. Streptavidin-phycoerythrin was added to each well and incubated at RT for 30 min. The magnetic beads were resuspended in sheath fluid and plate was assayed on spectrophotometer.

CXCL10 neutralization in vivo. RABV-infected mice were treated with 100 ug of anti-CXCL10 or isotype control antibody in 100 ul sterile PBS via the intraperitoneal route (i.p.) at 0, 2, and 4 days p.i. Sham-infected mice received 100 ul of sterile PBS as the control. Three mice were included in each group. At six days p.i., BBB permeability was determined by measuring NaF uptake as previously described. Data are expressed as the fold change in the amount of tracer in tissues by comparison with the values obtained for tissues from negative controls.

Statistical analysis. Data are expressed as mean \pm SEM and evaluation of the significance of differences between groups was performed by using student's t-test or using one-way analysis of variance (ANOVA) with Tukey's post hoc tests. $P < 0.05$ was considered as statistically significant in all studies. Graphs were plotted and analyzed using Graphpad Prism 5.0 (La Jolla, CA).

IV. Results

To determine the temporal and spatial expression of CXCL-10 in RABV infection, mice were infected with laboratory-attenuated (CVS-B2c) or wt (DRV-Mexico) RABV as described (6) and brains were harvested at days 3, 6, and 9 post-infection (p.i.). CXCL10 expressions in resident brain cells, specifically neurons, microglia, and astrocytes, were investigated using double-staining immunohistochemistry (IHC) with anti-CXCL10 antibody (R&D, Minneapolis, MN). Neurons, microglia, and astrocytes were respectively labeled with anti-NeuN (Chemicon, Germany), anti-Iba1 (Abcam, MA), and anti-GFAP (Abcam, MA) antibodies. The results are illustrated in Fig. 4.1. CXCL10 expression was detected in neurons as early as day 3 p.i. in mice infected with 10 50% lethal dose (LD₅₀) of CVS-B2c (Figs. 4.1A and 4.1B). CXCL10 expression was detected in neurons of mice infected with 1 and 10 LD₅₀ of CVS-B2c by day 6 p.i. and in mice infected with all the viruses by day 9 p.i.. CXCL10 expression was detected in microglia by day 6 (Figs. 4.1C and 4.1D) and in astrocytes by day 9 p.i. (Figs. 4.1E and 4.1F) after infection with each of the viruses. Overall significantly more CXCL10 was detected in mice infected with laboratory-attenuated than with wt RABV (Figs. 4.1B, 4.1D, and 4.1F). These data suggest that CXCL10 was initially expressed by neurons, then by microglia and astrocytes.

To ensure that these mice were infected with RABV, virus antigens were detectable by using anti-RABV nucleoprotein (N) antibodies (6). Sporadic antigen expression was detected in the brain of mice infected with CVS-B2c by day 3 p.i.. A significantly higher expression of RABV antigen was detected in brain of mice infected with CVS-B2c at days 6 and 9 p.i. (Figs.

4.1G and 4.1H). Only sporadic RABV antigen was detected in the brain of mice infected with wt RABV even at day 9 p.i.

In RABV infection, it has been shown that CD4⁺ T, but not CD8⁺ T or B, cells are required to enhance BBB permeability (22). It has been demonstrated that CXCR3⁺CD4⁺ T cells differentiating into IL17-producing Th17 and IFN- γ -producing Th1 cells is the exclusive mechanism of leukocyte skewing in the CNS inflammation (23). IL17 has been reported to be a crucial determinant for tight junction (TJ) protein alteration and BBB disruption (24). To determine that Th17 cells are differentiated from CXCR3⁺CD4⁺ T cells in RABV infection, Th17 cells were detected by using CD4 and IL17 as the cell markers (25). As shown in Fig. 4.2, double-labeling of CD4 and IL17 was found in the brain of mice infected with high dose CVS-B2c at day 6 p.i. (Fig. 4.2). By day 9 p.i., CD4⁺IL17⁺ cells were detected in all infected animals although significantly more Th17 cells were detected in CVS-B2c- than DRV-Mexico-infected mice (Fig. 4.2). The infiltration of CD4⁺IL17⁺ cells coincides with the enhancement of BBB permeability (6) in these animals, indicating that enhancement of BBB permeability is associated with the IL17-expressing Th17 cells differentiated from CD4⁺ T cells in RABV infection. Since CXCL10 is one of the earliest chemokines expressed after infection with laboratory-attenuated RABV (day 3 p.i.), it could have played a pivotal role in directing and promoting the infiltration of CXCR3⁺CD4⁺ T cells into the CNS of mice infected with RABV (23).

In our previous studies, IFN- γ was detected in the late stage of RABV infection (6). It is possible that CXCL10-recruited CXCR3⁺CD4⁺ T cells in the CNS express IFN- γ , which magnifies CXCL10 production, consequently initiating a full-blown inflammatory response and

resulting in enhancement of BBB permeability (26, 27). Indeed, neutralization of IFN- γ resulted in the amelioration of inflammation and BBB permeability enhancement (6). However, the temporal and spatial pattern of CXCL10 and IFN- γ expression suggest that CXCL10 is the initiation, while IFN- γ is the amplification factor for inflammation and BBB enhancement. To confirm this notion, female ICR mice were divided into three groups: a control group; a group receiving 10LD₅₀B2c at day 0 via the intracranial route and 100 ng anti-CXCL10 antibody at day 0, 2, and 4 via the intraperitoneal route; a third group receiving 10LD₅₀B2c and three treatments of isotype-control antibody. At day 6 p.i., BBB permeability in these mice was determined by NaF uptake as described previously (6). Briefly, NaF was used as the tracer; 100 μ l of 100 mg/ml NaF was injected into each mouse through the tail vein. Peripheral blood was collected after circulation for 10 min, serum and phosphate-buffered saline (PBS)-perfused brains were then harvested. The amount of NaF taken up into brain tissues is expressed as micrograms of fluorescence per milligram of cerebrum or cerebellum, divided by the micrograms of fluorescence per microliter of serum in order to normalize for the amounts of tracer taken up from peripheral blood at the time of brain tissue collection (22). It was found that anti-CXCL10 antibody significantly reduced the enhancement of BBB permeability in CVS-B2c-infected mice when compared to mice receiving isotype control antibodies (Fig. 4.3A). Expressions of IFN- γ in homogenized brain samples derived from three groups were assessed using ELISA (Biolegend, CA). As shown in Fig. 4.3B, significantly lower level of IFN- γ was detected in RABV-infected groups treated with anti-CXCL10 antibodies than that in the group treated with isotype control antibodies. Consistently, fewer Th17 cells were found in the brains of mice infected with RABV and treated with anti-CXCL10 antibodies than that in those of mice treated with isotype control

antibodies (Figs. 4.3C and 4.3D). These results indicate that neutralization of CXCL10 resulted in amelioration of BBB disruption, reduction of IFN- γ expression and infiltration of Th17 cells into the CNS.

To confirm these findings, mouse brain microvascular endothelial cells (MBMECs), bEnd.3, was cultured and inoculated with brain homogenates (50 μ l) prepared from mice infected with laboratory-attenuated RABV and treated with anti-CXCL10 or with isotype-control antibodies for 24 h at 37°C. The expression of occludin was determined using Western blotting (WB) and confocal microscopy as previously described (6). MBMECs co-cultured with brain extract prepared from mice treated with CXCL10 antibodies showed significantly higher level of occludin expression than in cells treated with brain extract derived from mice treated with isotype control antibodies as detected by WB (Figs. 4.4A and 4.4B) and confocal microscopy (Figs. 4.4C and 4.4D). These results further confirm that CXCL10 initiates the cascade, leading to infiltration of inflammatory cells, up-regulation of IFN- γ and down-regulation of TJ protein expression, which consequently results in enhanced BBB permeability in RABV infection.

V. Discussion

Our previous studies demonstrated that it is the chemokines/cytokines induced by RABV infection responsible for reduction of TJ protein expression and the enhancement of BBB permeability (6). Indeed, depleting one of the cytokines, IFN- γ , with antibodies ameliorated the reduction of TJ protein expression in infected MBMECs and the enhancement of BBB permeability in infected mice. However, the up-regulation of IFN- γ occurred at the later stage of

RABV infection (day 9 p.i.) and CXCL10, was up-regulated the most and earliest post infection, leading us to hypothesize that CXCL10 might be the initiation factor for the eventual enhancement of BBB permeability in mice infected with RABV. In the present study, we show that the expression of CXCL10 can be detected as early as day 3 after infection. Neutralizing CXCL10 reduced the expression of IFN- γ , restored the expression TJ proteins, and ameliorated the enhancement of BBB permeability. These results together demonstrate that indeed CXCL10 initiates the cascades leading to expression of other inflammatory chemokines/cytokines, reduction of TJ protein expression, and enhancement of the BBB permeability during RABV infection.

CXCL10 is an IFN- γ inducible protein and binds to receptor CXCR3 expressed on activated CD4⁺ T cells and functions in governing migration of lymphocytes into the CNS (8). CXCL10 attracts CXCR3⁺CD4⁺ T cells infiltrating into the CNS along the chemokine gradient and differentiating to IL-17-producing Th17 cells and IFN- γ -producing Th1 cells (23). As we have hypothesized previously that IFN- γ secreted by Th1 cells promotes the positive feedback, amplifies CXCL10 production, and CXCR3⁺CD4⁺ T cells influx into the CNS in the RABV infection (10). IL-17 produced by Th17 cells in the CNS initiates the alteration of TJ proteins (24). Both Th1 and Th17 cells work in concert, leading to the breakdown of the BBB in the RABV infection. Indeed the expression of IL17 was found to be expressed significantly more in the brain of mice infected with laboratory-attenuated than wt RABV, at day 6 p.i., corresponding to the enhancement of BBB permeability (6). In the present study, neutralization of CXCL10 reduced the expression of both IFN- γ and IL17, which consequently ameliorates the enhancement of BBB permeability. Neutralization of CXCL10 has also been reported to reduced

BBB disruption and infiltration of immune cells in the CNS in an EAE animal model (18, 19). In West Nile virus (WNV) infection, depletion of CXCL10 decreased the number of CXCR3+CD8+ T cells infiltrating into the brain (9).

CXCL10 can be secreted by brain resident cells such as neurons, microglial cells, and astrocytes; it can also be produced by immune cells influx from the periphery. Our temporal and spatial studies indicate that the earliest CXCL10 expression was detected in neurons (day 3 p.i.), then microglia (day 6 p.i.), and finally in astrocytes (day 9 p.i.). Although the mechanism(s) by which RABV infection induces the CXCL10 expression remains unclear, it is tempting to speculate that it is the neuronal CXCL10 activates other neural resident cells (expression of CXCL10 and other chemokines/cytokines) as well as attract infiltration of inflammatory cells into the CNS. CXCL10 has been found to be expressed in WNV infection and it is believed that neuronal CXCL10 initiates influx of CD8+ T cells into the CNS (9).

Fig. 4.1

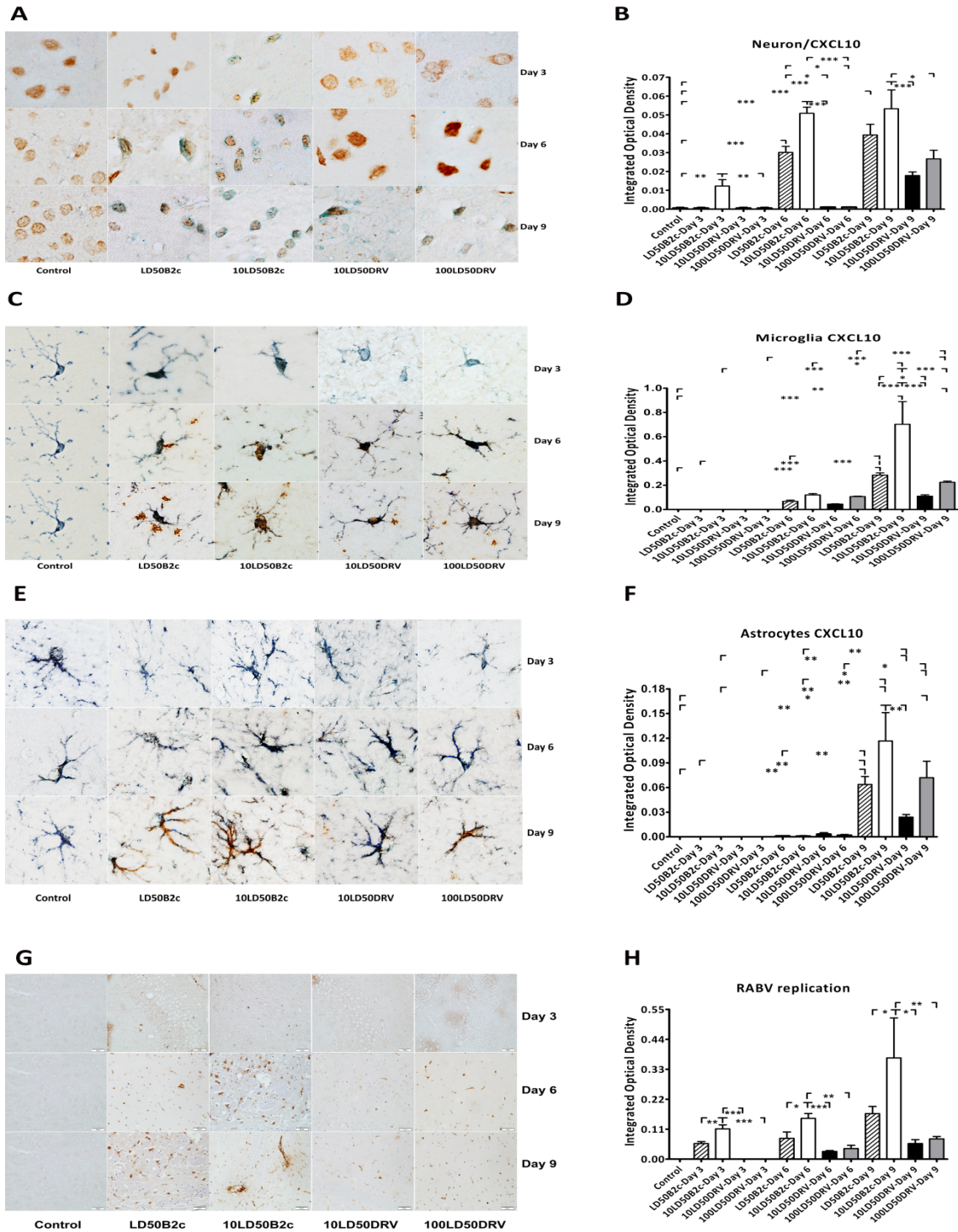


Fig. 4.1. CXCL10 was initially detected in neurons before in microglia and astrocytes. Mice were infected i.c. with 1 or 10 LD₅₀ of CVS-B2c, 10 or 100 LD₅₀ of DRV-Mexico. At day 3, 6 or 9 p.i., animals were euthanized and brains were harvested, fixed, and sectioned for measuring the CXCL10 expression in brain cells using double-labeling IHC with antibodies to respective cell markers. (A) Co-localization of CXCL10 (blue) and Neuron-N proteins (blue). (C) Co-localization of CXCL10 (brown) with Iba-1 protein (microglia, blue). (D) Co-localization of CXCL10 (brown) with GFAP protein (astrocytes, blue). (G) RABV load was shown both in laboratory-attenuated and wt RABV-infected mice. (B, D, F, and G) Statistical analysis of expression of CXCL10 in brain resident cells. Data are presented as mean ± SEM from three independent experiments. Statistics in panels are repeated-measure ANOVA with Tukey's post hoc test, asterisk indicate the statistical significance. *, P < 0.05; **, P < 0.01; ***, P < 0.001; ****, P<0.0001.

Fig 4.2

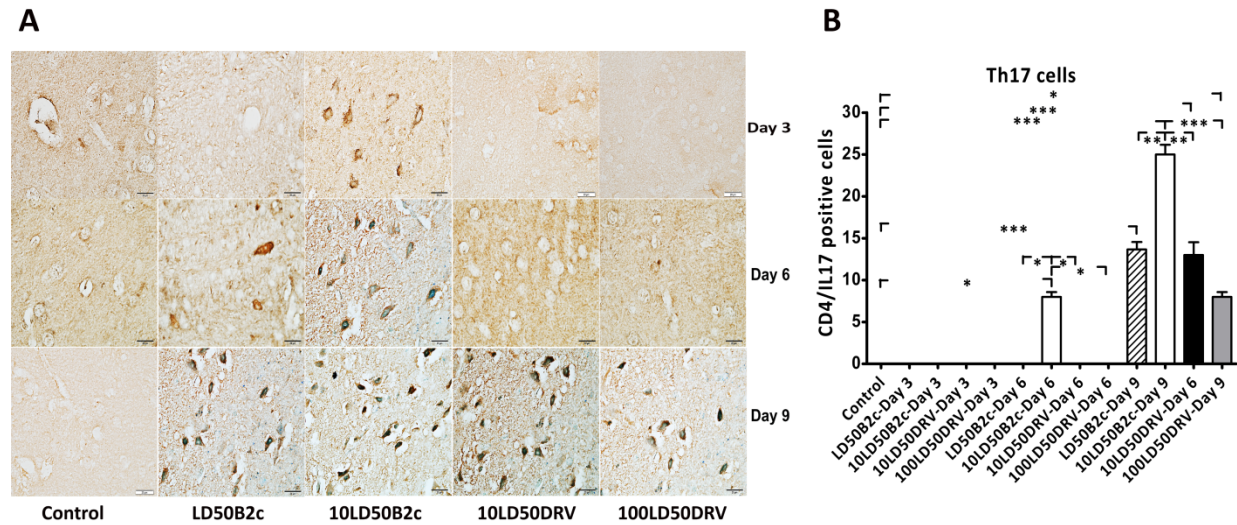


Fig. 4.2. Significantly more Th17 cells were observed in laboratory-attenuated- than wt-RABV-infected mice brains. Mice were infected i.c. with 1 or 10 LD₅₀ of CVS-B2c, 10 or 100 LD₅₀ of DRV-Mexico. At day 3, 6 or 9 p.i., animals were euthanized and brains were harvested, fixed, and sectioned for measuring the Th17 cell number using double-labeling IHC. (A) Colocalization of IL17 (blue) and CD4 (brown) cell markers. (B) Statistical analysis of Th17 cell number in RABV-infected brains. Data are presented as mean ± SEM from three independent experiments. Statistics in panels are repeated-measure ANOVA with Tukey's post hoc test, asterisk indicate the statistical significance. *, P < 0.05; **, P < 0.01; ***, P < 0.001; ****, P<0.0001.

Fig. 4.3

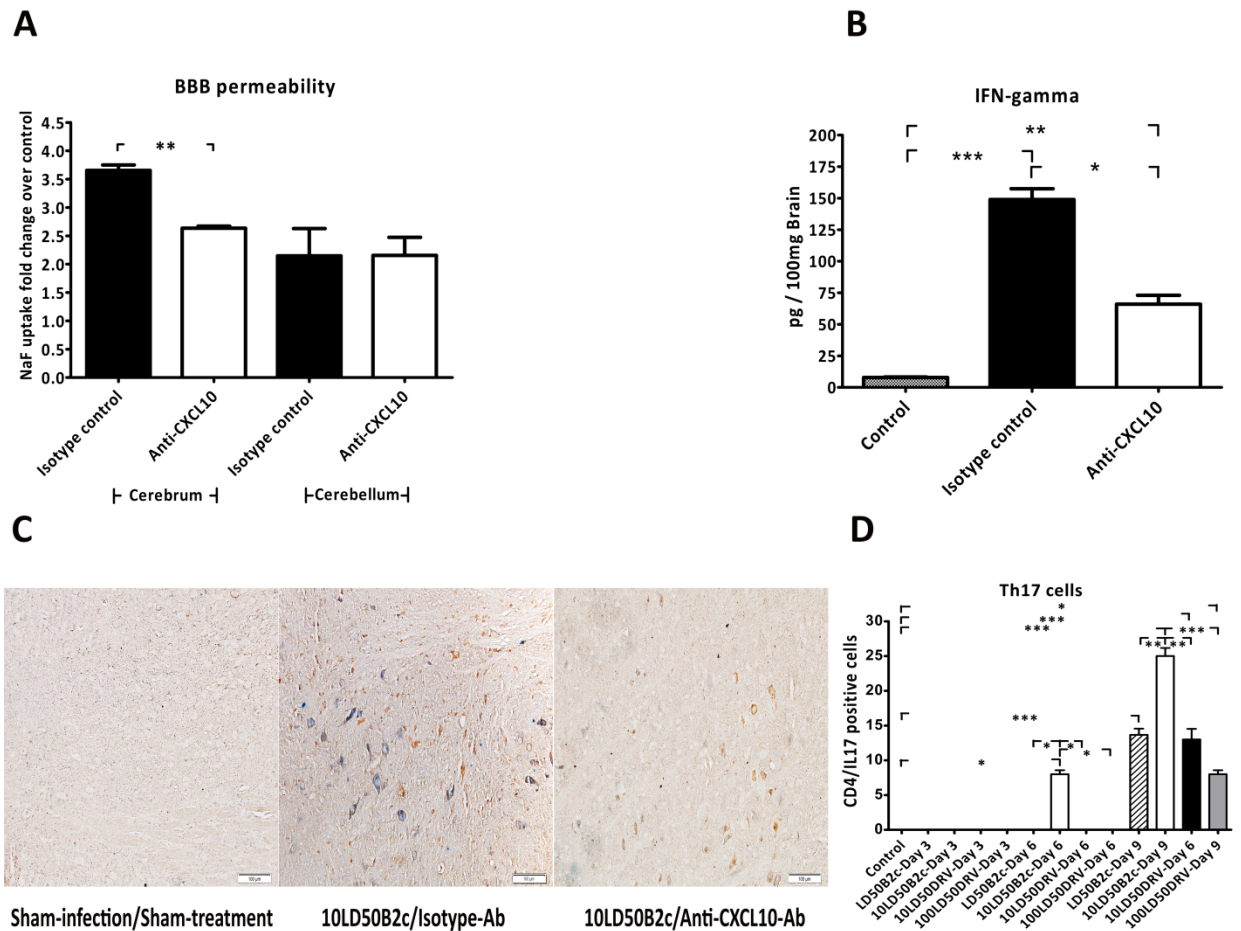


Fig. 4.3. Neutralization of CXCL10 in RABV-Infected mice. Female ICR mice infected i.c. with 10 LD₅₀ of CVS-B2c were injected i.p. with 100 ug anti-CXCL10 neutralizing antibody or isotype control antibody in PBS at 0, 2, and 4 days p.i.. At day 6 p.i., BBB permeability was assessed by NaF uptake in the cerebrum and the cerebellum (A). (B) Expression of IFN- γ in mice brains. (C) Neutralization of CXCL10 reduced the Th17 cell number in RABV-infected

brain. (D) Data are presented as mean \pm SEM from three independent experiments. Statistics in panel D is repeated-measure ANOVA with Tukey's post hoc test, asterisk indicate the statistical significance. *, P < 0.05; **, P < 0.01; ***, P < 0.001; ****, P<0.0001.

Fig. 4.4

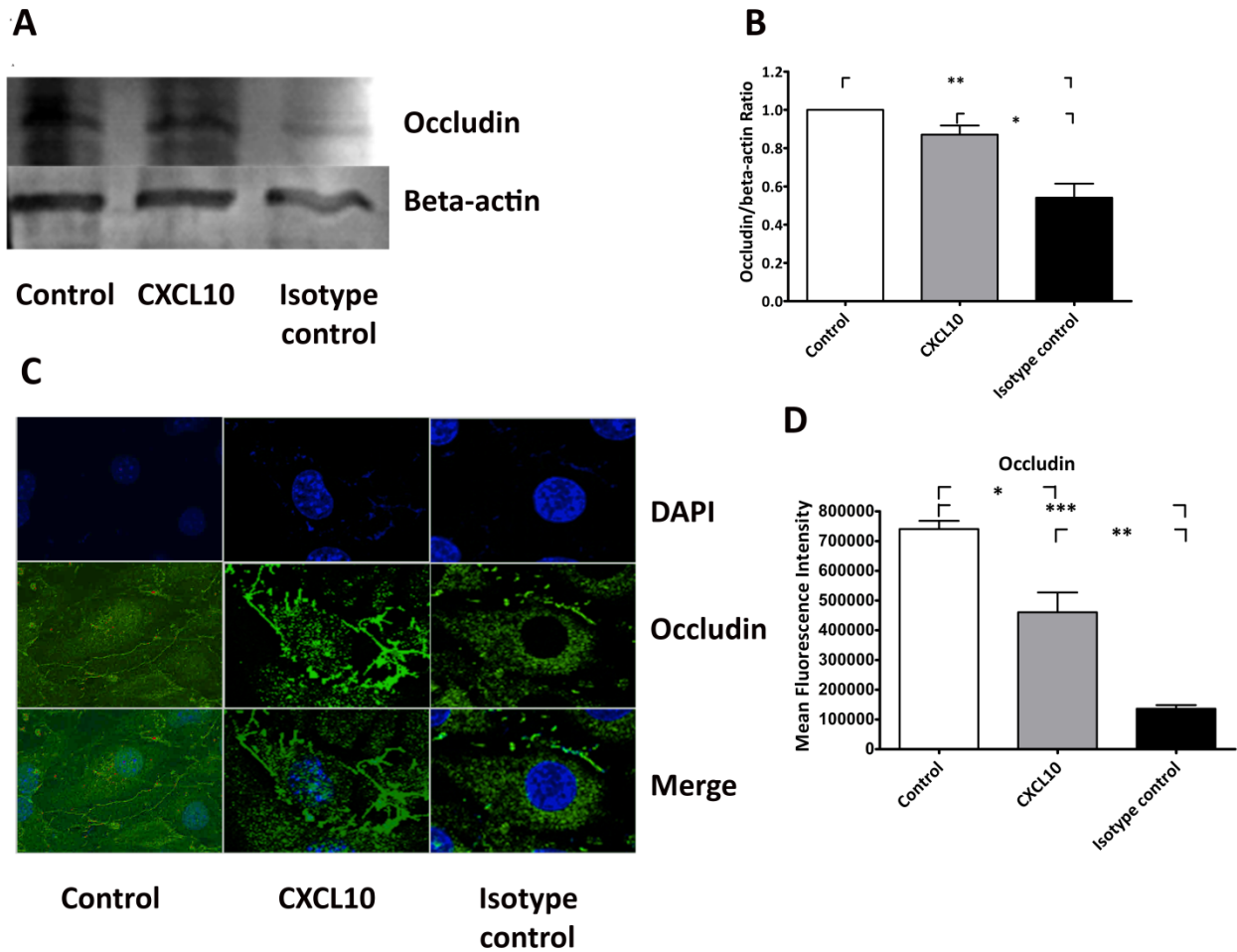


Fig. 4.4 Neutralization of CXCL10 rescued the expression level of TJ protein in RABV-infected mice. The expression of occludin in BMECs after co-culturing with brain extracts was also detected using quantitative Western blotting (A). Quantitative Western blotting analyses of TJ protein expressions in BMECs treated with brain extracts derived from mice infected with CVS-B2c and treated with either antibody (anti-CXCL10 or isotype control), bEnd.3 cells treated with brain extracts derived from sham-infected mice were the control (B). Mouse BMECs were co-cultured with brain extracts (treated with DMEM, anti-CXCL10 antibody, or isotype control

antibody) derived from mice infected with 10LD₅₀ of CVS-B2c. After 24 h, BMECs were fixed and stained with DAPI and anti-claudin-5 antibody or DAPI and anti-occludin antibody. The staining was visualized by confocal microscopy. Panel C shows the MFI at ROI drawn around the cells under each condition (C). (D) Data are presented as mean ± SEM from three independent experiments. Statistics in panel D repeated-measure ANOVA with Tukey's post hoc test, asterisk indicate the statistical significance. *, P < 0.05; **, P < 0.01; ***, P < 0.001; ****, P < 0.0001.

VI. References

1. Fu ZF. 1997. Rabies and rabies research: past, present and future. *Vaccine* 15 Suppl:S20-24.
2. World Health O. 2013. WHO Expert Consultation on Rabies. Second report. World Health Organization technical report series:1-139, back cover.
3. Wang ZW, Sarmiento L, Wang Y, Li XQ, Dhingra V, Tseggai T, Jiang B, Fu ZF. 2005. Attenuated rabies virus activates, while pathogenic rabies virus evades, the host innate immune responses in the central nervous system. *Journal of virology* 79:12554-12565.
4. Roy A, Phares TW, Koprowski H, Hooper DC. 2007. Failure to open the blood-brain barrier and deliver immune effectors to central nervous system tissues leads to the lethal outcome of silver-haired bat rabies virus infection. *Journal of virology* 81:1110-1118.

5. Hooper DC, Phares TW, Fabis MJ, Roy A. 2009. The production of antibody by invading B cells is required for the clearance of rabies virus from the central nervous system. *PLoS neglected tropical diseases* 3:e535.
6. Chai Q, He WQ, Zhou M, Lu H, Fu ZF. 2014. Enhancement of blood-brain barrier permeability and reduction of tight junction protein expression are modulated by chemokines/cytokines induced by rabies virus infection. *Journal of virology* 88:4698-4710.
7. Nagpal ML, Davis J, Lin T. 2006. Overexpression of CXCL10 in human prostate LNCaP cells activates its receptor (CXCR3) expression and inhibits cell proliferation. *Biochimica et biophysica acta* 1762:811-818.
8. Nakajima C, Mukai T, Yamaguchi N, Morimoto Y, Park WR, Iwasaki M, Gao P, Ono S, Fujiwara H, Hamaoka T. 2002. Induction of the chemokine receptor CXCR3 on TCR-stimulated T cells: dependence on the release from persistent TCR-triggering and requirement for IFN-gamma stimulation. *European journal of immunology* 32:1792-1801.
9. Klein RS, Lin E, Zhang B, Luster AD, Tollett J, Samuel MA, Engle M, Diamond MS. 2005. Neuronal CXCL10 directs CD8+ T-cell recruitment and control of West Nile virus encephalitis. *Journal of virology* 79:11457-11466.
10. Luster AD, Ravetch JV. 1987. Biochemical characterization of a gamma interferon-inducible cytokine (IP-10). *The Journal of experimental medicine* 166:1084-1097.
11. Harikumar KB, Yester JW, Surace MJ, Oyeniran C, Price MM, Huang WC, Hait NC, Allegood JC, Yamada A, Kong X, Lazear HM, Bhardwaj R, Takabe K, Diamond MS, Luo C, Milstien S, Spiegel S, Kordula T. 2014. K63-linked polyubiquitination of transcription factor

IRF1 is essential for IL-1-induced production of chemokines CXCL10 and CCL5. *Nature immunology* 15:231-238.

12. Singh UP, Singh S, Singh R, Cong Y, Taub DD, Lillard JW, Jr. 2008. CXCL10-producing mucosal CD4⁺ T cells, NK cells, and NKT cells are associated with chronic colitis in IL-10(-/-) mice, which can be abrogated by anti-CXCL10 antibody inhibition. *Journal of interferon & cytokine research : the official journal of the International Society for Interferon and Cytokine Research* 28:31-43.

13. Nakamichi K, Inoue S, Takasaki T, Morimoto K, Kurane I. 2004. Rabies virus stimulates nitric oxide production and CXC chemokine ligand 10 expression in macrophages through activation of extracellular signal-regulated kinases 1 and 2. *Journal of virology* 78:9376-9388.

14. Asensio VC, Campbell IL. 1997. Chemokine gene expression in the brains of mice with lymphocytic choriomeningitis. *Journal of virology* 71:7832-7840.

15. Asensio VC, Maier J, Milner R, Boztug K, Kincaid C, Moulard M, Phillipson C, Lindsley K, Krucker T, Fox HS, Campbell IL. 2001. Interferon-independent, human immunodeficiency virus type 1 gp120-mediated induction of CXCL10/IP-10 gene expression by astrocytes in vivo and in vitro. *Journal of virology* 75:7067-7077.

16. Lane TE, Asensio VC, Yu N, Paoletti AD, Campbell IL, Buchmeier MJ. 1998. Dynamic regulation of alpha- and beta-chemokine expression in the central nervous system during mouse hepatitis virus-induced demyelinating disease. *Journal of immunology* 160:970-978.

17. Liu MT, Keirstead HS, Lane TE. 2001. Neutralization of the chemokine CXCL10 reduces inflammatory cell invasion and demyelination and improves neurological function in a viral model of multiple sclerosis. *Journal of immunology* 167:4091-4097.

18. Fife BT, Kennedy KJ, Paniagua MC, Lukacs NW, Kunkel SL, Luster AD, Karpus WJ. 2001. CXCL10 (IFN-gamma-inducible protein-10) control of encephalitogenic CD4+ T cell accumulation in the central nervous system during experimental autoimmune encephalomyelitis. *Journal of immunology* 166:7617-7624.
19. Wildbaum G, Netzer N, Karin N. 2002. Plasmid DNA encoding IFN-gamma-inducible protein 10 redirects antigen-specific T cell polarization and suppresses experimental autoimmune encephalomyelitis. *Journal of immunology* 168:5885-5892.
20. Narumi S, Kaburaki T, Yoneyama H, Iwamura H, Kobayashi Y, Matsushima K. 2002. Neutralization of IFN-inducible protein 10/CXCL10 exacerbates experimental autoimmune encephalomyelitis. *European journal of immunology* 32:1784-1791.
21. Klein RS, Izikson L, Means T, Gibson HD, Lin E, Sobel RA, Weiner HL, Luster AD. 2004. IFN-inducible protein 10/CXC chemokine ligand 10-independent induction of experimental autoimmune encephalomyelitis. *Journal of immunology* 172:550-559.
22. Phares TW, Fabis MJ, Brimer CM, Kean RB, Hooper DC. 2007. A peroxynitrite-dependent pathway is responsible for blood-brain barrier permeability changes during a central nervous system inflammatory response: TNF-alpha is neither necessary nor sufficient. *Journal of immunology* 178:7334-7343.
23. Shechter R, London A, Schwartz M. 2013. Orchestrated leukocyte recruitment to immune-privileged sites: absolute barriers versus educational gates. *Nature reviews. Immunology* 13:206-218.
24. Huppert J, Closhen D, Croxford A, White R, Kulig P, Pietrowski E, Bechmann I, Becher B, Luhmann HJ, Waisman A, Kuhlmann CR. 2010. Cellular mechanisms of IL-17-induced

blood-brain barrier disruption. *FASEB journal : official publication of the Federation of American Societies for Experimental Biology* 24:1023-1034.

25. Tzartos JS, Friese MA, Craner MJ, Palace J, Newcombe J, Esiri MM, Fugger L. 2008. Interleukin-17 production in central nervous system-infiltrating T cells and glial cells is associated with active disease in multiple sclerosis. *The American journal of pathology* 172:146-155.

26. Muller M, Carter S, Hofer MJ, Campbell IL. 2010. Review: The chemokine receptor CXCR3 and its ligands CXCL9, CXCL10 and CXCL11 in neuroimmunity--a tale of conflict and conundrum. *Neuropathology and applied neurobiology* 36:368-387.

27. Whiting D, Hsieh G, Yun JJ, Banerji A, Yao W, Fishbein MC, Belperio J, Strieter RM, Bonavida B, Ardehali A. 2004. Chemokine monokine induced by IFN-gamma/CXC chemokine ligand 9 stimulates T lymphocyte proliferation and effector cytokine production. *Journal of immunology* 172:7417-7424.

CHAPTER 5

SUMMARY AND DISCUSSION

In the present studies, mechanism of BBB permeability enhancement was investigated by comparing the disparities of wt and laboratory-attenuated RABVs. It was found that BBB disruption and reduction of TJ protein expressions in laboratory-attenuated RABV infected animal is due to chemokines/cytokines expression and the process of BBB disruption is initiated by CXCL10 expressed by neurons and amplified by cascades of other inflammatory chemokines/cytokines expressions.

The rationale to investigate the effect of chemokines/cytokines on the BBB was based on our previous findings that laboratory-attenuated RABV induces innate and adaptive immunity, while wt RABV evades immune surveillance. It has also been shown in our previously studies that disrupted BBB after infection with laboratory-attenuated RABV allows immune effectors (immune cells and VNA) to enter the CNS and clear the established infection, while intact BBB is observed concurrently with no immune cells influx in wt RABV-infected animals. It was found that high levels of chemokines/cytokines in laboratory-attenuated RABV infection interrupted BBB permeability and reduced TJ protein expressions both *in vivo* and *in vitro*. Neutralization of one of the chemokines (IFN- γ) significantly reduced the loss of TJ proteins and BBB disruption. No change in TJ protein expression was observed when virus was

inoculated onto endothelial cell monolayer. Thus enhancement of BBB permeability and reduction of TJ proteins is due to expression of chemokines/cytokines induced by laboratory-attenuated RABV infection, but not due to direct damage caused by the virus per se.

Previous studies in our laboratory demonstrated that expression of CXCL10 was best correlated with influx of immune cells into the CNS and enhancement of BBB permeability when it was compared with other chemokines, such as CCL5 and CCL3. CXCL10 was found to be the earliest and most highly expressed chemokine in mice infected with laboratory-attenuated RABV in the present study. Although CXCL10 can be stimulated by expression of IFN- γ , its expression occurred later than that of CXCL10. CXCL10 was found initially in neurons before it became detectable in microglia and astrocytes. These results indicate that it is neuronal CXCL10 that initiates the cascade of BBB permeability enhancement. IFN- γ may amplify the enhancement of BBB permeability. Neutralization of CXCL10 substantially restored TJ protein expression, and reduced IFN- γ expression and ameliorated the enhancement of BBB permeability.

Amplification of BBB permeability enhancement was investigated in laboratory-attenuated RABV infected animals. We hypothesized that chemokines/cytokines produced by infiltrated immune cells contributed to amplifying the positive feedback loop of BBB disruption. It was found that laboratory-attenuated RABV infection stimulated significantly more immune cells infiltrating the CNS than wt RABV infection. It has been demonstrated that CXCR3+CD4+ T cells can differentiate into IL17-producing Th17 cells and IFN- γ -producing Th1 cells in the CNS infection. Significantly more Th17 cells were found in animals infected with laboratory-

attenuated than with wt RABV, and neutralization of CXCL10 reduced the Th17 cell number in laboratory-attenuated RABV infected animals. Together these data indicate that CXCR3+CD4+ T cells recruited by CXCL10 enter the CNS, induce a full blown inflammation, and amplify enhancement of BBB permeability in RABV infection.

BBB has been considered as a target for therapeutic purposes in fighting diseases in the CNS. Deliberate transient disruption of TJ proteins and opening of the BBB are commonly studied in order to facilitate drug delivery through the brain endothelium, although disruption of BBB integrity needs to be a brief and practical process to reduce edema, autoimmune disease, extensive inflammation, and other side effects. In tumor therapy, intracarotid infusion of hyperosmolar solution crossing the disrupted BBB has shown promising success in delivering chemotherapy in fighting brain tumor. In the present study, we demonstrated that enhancement of BBB permeability and reduction of TJ protein expressions in RABV infection are modulated by chemokine/cytokine expression, and the cascades of BBB disruption is initiated by neuronal CXCL10 and amplified by induction of downstream chemokines/cytokines such as INF- γ . Therefore, chemokines, especially CXCL10, might be considered as candidates in opening up the BBB, delivering immune effectors, and rescuing animals from established RABV infections.